

CLIP’s Visual Embedding Projector is a Few-shot Cornucopia

Mohammad Fahes¹ Tuan-Hung Vu^{1,2} Andrei Bursuc^{1,2} Patrick Pérez³ Raoul de Charette¹
¹ Inria ² Valeo.ai ³ Kyutai

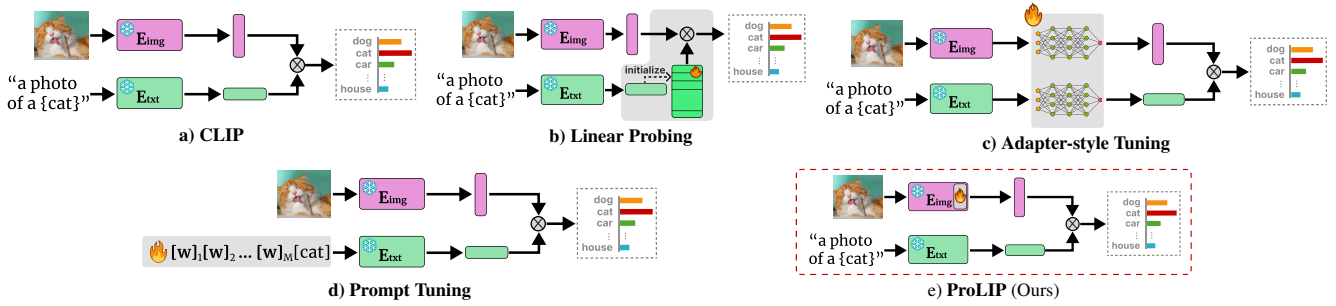


Figure 1. **Few-shot classification with CLIP.** a) Using a pre-trained CLIP, *zero-shot* classification is performed by measuring text and visual embeddings similarity. Among *few-shot* adaptation strategies of CLIP, b) Linear Probing [19, 38] trains a linear classifier of the visual features, c) Adapter-style tuning adds external learnable MLPs [11, 51], d) Prompt Tuning learns word embeddings [5, 54–56]. Alternatively, we propose e) ProLIP which does not introduce new weights and only fine-tunes the visual embedding projector.

Abstract

We consider the problem of adapting a contrastively pre-trained vision-language model like CLIP [32] for few-shot classification. The literature addresses this problem by learning a linear classifier of the frozen visual features, optimizing word embeddings, or learning external feature adapters. We introduce an alternative way for few-shot CLIP adaptation without adding “external” parameters to optimize. We find that simply fine-tuning the embedding projection matrix of the vision encoder leads to better performance than all baselines. Furthermore, we show that regularizing training with the distance between the fine-tuned and pretrained matrices adds reliability for adapting CLIP, making the results stable across different learning rates in the “validation-free” setting. This simple approach, coined ProLIP, yields state-of-the-art performance on 11 few-shot classification benchmarks, few-shot cross-dataset transfer, domain generalization, and base-to-new class generalization. We also show that ProLIP significantly outperforms prompt tuning when extended to another task of test-time adaptation, while being one order of magnitude faster to train. Code will be made available at: <https://github.com/astra-vision/ProLIP>.

1. Introduction

Contrastive Language-Image Pretraining (CLIP) [32] has shown that strong visual features can be learned from noisy

natural language descriptions at *very* large scale. The true potential of CLIP lies in its shared vision-text space, breaking the long-standing constraints of closed-set systems and enabling non-trivial interactions and querying between text and images via prompts. Such a freedom in the label space makes the model readily applicable to a wide range of specialized downstream applications.

CLIP trains a vision and a text encoder on large batches of image-text pairs using a sum of contrastive image-to-text and text-to-image losses. At inference, given an image and a set of classes expressed within prompts (e.g., “a photo of {class_k}”), one can perform *zero-shot classification*. The predicted class is simply the one for which the textual embedding has the highest similarity with the image embedding. The prompt template can be engineered to boost the zero-shot performance, or automated by querying multiple descriptors of a class from Large Language Model (LLMs) [3, 28]. Yet, the zero-shot performance may still be unsatisfactory, especially for data that are supposedly underrepresented in CLIP’s training data. Examples of such cases include geospatial data, e.g., EuroSAT [14] and specialized data, e.g., FGVCaircraft [27]. Thus, a practical setting emerged in transfer learning: *Given a labeled few-shot training dataset of images, how to efficiently adapt CLIP in order to maximize the performance on the test set?*

Hinging on only a few labeled samples for supervision, model training is prone to overfitting. The common strategy is to avoid full fine-tuning and instead adapt only a few parameters [23]. Starting from a concept-rich pretrained CLIP

model, such parameter-efficient strategies have been shown to be effective for few-shot tasks. In this direction, the literature explores three avenues schematized in Fig. 1. First, prompt tuning [54, 55] replaces the template with learnable parameters in the word embedding space, while freezing both vision and text encoders. Second, CLIP adapters [11] learn a multi-layer perceptron (MLP) on top of the frozen visual or text features, and use a residual connection aiming at partially using the zero-shot features. In these two paradigms, the text embeddings are used as classification weights. Third, linear probing (LP) [32] simply trains a linear classifier on top of the frozen visual features.

While technically simple and parameter-efficient, existing solutions still have limitations. Prompt tuning methods [5, 55, 56] are slow to train as gradients need to be backpropagated over the entire text encoder. In addition, varying context lengths and class-name positions affect performance. Adapters [11, 51] impose architectural choices of the MLP, the bottleneck dimension and the residual connection. Linear probing methods [19, 26, 32, 38] cannot be applied to open-class and cross-dataset transfer settings since the classifier is restricted to few-shot training classes.

The previous methods either train “external” parameters (Adapters, LP), or learn parameters in the input space (prompt tuning). To the best of our knowledge, no existing work tackles few-shot CLIP adaptation problem with parameter-efficient fine-tuning of the model weights. In this work, we propose the first baseline for model-weight-based few-shot learning. Our method, dubbed “ProLIP”, is both extremely simple to implement, being only a few lines of code, and very effective: *considering pretrained visual and text CLIP encoders f and g , we fine-tune the embedding projection matrix of f (i.e., the projector that maps visual embeddings into the shared embedding space) with a cross-entropy loss while constraining its weights to remain close to the pretrained ones through a regularization loss.* Fig. 1 illustrates existing approaches and our proposed ProLIP, which is further detailed in Sec. 4.

ProLIP is advantageous for a number of reasons:

- It alleviates the need of “external” parameters, avoiding network design search and heavy hyperparameter tuning.
- Training only the embedding projector is fast, requiring up to 2 seconds on saved pre-projection features.
- ProLIP uses CLIP’s native text embeddings as classification weights and thus preserves its open-class capability.
- ProLIP maintains stable performance across various learning rates. ProLIP thus works well in the fair and realistic *few-shot validation* [19] and *validation-free* [38] settings when there are only a few or no validation samples used for hyperparameter tuning.
- ProLIP extends to the task of test-time adaptation.

Our simple method performs on par with or better than the literature on few-shot adaptation, few-shot cross-dataset

generalization, domain generalization, and base-to-new class generalization. Additionally, ProLIP significantly outperforms prompt tuning in test-time adaptation, which is an unsupervised learning setting, while being one order of magnitude faster to train.

2. Related work

Parameter-efficient fine-tuning (PEFT). The advent of increasingly larger pretrained vision foundation models with strong generalization enables transfer learning approaches using limited labeled data. Full fine-tuning is computationally inefficient, yet often underperforming even when compared to linear probing [23, 44]. PEFT methods aim to adapt models effectively with minimal parameter updates. Side-tuning [50] trains a small parallel network to prevent catastrophic forgetting. Optimizing only certain parameters, such as bias terms [48], is also effective; however, this still requires full backpropagation. Adapter-tuning methods introduce adaptation modules to transformer blocks [17, 35], but incur a higher runtime cost. LoRA [18] optimizes new low-rank matrices injected into transformer layers to approximate weight changes during fine-tuning, significantly reducing the number of parameters to learn. Prompt-tuning, such as VPT [20], adds learnable prompts to input patch embeddings. In addition to the computational overheads, these methods are specifically devised for transformers and are not directly applicable to convolutional networks.

Few-shot CLIP adaptation. CLIP’s specific interaction between text and image features has enabled new adaptation methods that leverage this property, especially in few-shot scenarios. Inspired by prompt tuning in natural language processing [25, 53], Zhou et al. [55] proposed context optimization (CoOp) which applies the same concept for pretrained vision-language models. CoOp was later shown not to generalize well on unseen classes within the same dataset. Thus, conditional context Optimization (CoCoOp) [54] adds a meta-network that generates input-conditional tokens in addition to the learnable vectors, making optimized context less prone to overfitting to the seen classes. Zhu et al. [56] highlighted that unconstrained prompt tuning can lead to overfitting in low-shot settings, reducing zero-shot performance. They proposed regularizing training by updating only prompts whose gradients align with zero-shot predictions. PLOT [5] applies optimal transport on sets of text and visual features to learn the transport plan between the two sets in an inner loop, which is fixed in the outer loop where prompts are learned. MaPLe [21] learns prompts in both vision and text branches at input and intermediate layers with a coupling function.

A simple approach for few-shot CLIP adaptation is to train a linear probe on top of the visual features [32]. Lin

et al. [26] show that adding a text describing the class to the training data of few-shot images largely boosts linear probing. Huang et al. [19] blend text embeddings with classification weights using class-wise learnable parameters.

Instead of adapting the model in the input space or training a linear probe, CLIP-adapter [11] adds an MLP on top of the features in the shared embedding space, with a residual connection to preserve the pretrained knowledge. Zhang et al. [51] create a training-free cache-model from the visual features of the few-shot training set, which are converted into the weights of the MLP adapter. Also training-free, [43] ensembles the zero-shot classifiers with Gaussian Discriminative Analysis (GDA) [1], which assumes that features of each class follow Gaussian distributions. CLIPood [37] fine-tunes the full encoder with a beta moving average regularization to keep the updated weights close to zero-shot ones. Of note, we fine-tune only the embedding projector with 0.45% of parameters compared to CLIPood, and use a simpler regularization.

Some works leverage external priors to boost the few-shot performance. For instance, APE [57] uses GPT-3 to generate descriptions, CaFo [52] uses GPT-3 [3], DINO [4], and DALL-E [33], while AMU-tuning [40] presents a unified view on few-shot adaptation strategies from a logit bias perspective and uses MoCov3 [6] as additional prior. Our work belongs to the category harnessing only the CLIP model with no extra information [19, 21, 38, 47, 51].

3. Preliminaries

3.1. Zero-shot classification

We denote f and g the vision and text encoders of CLIP, respectively. During pretraining, CLIP learns a joint embedding space that pulls corresponding image-text representations closer together and pushes away dissimilar ones. At inference, given an image \mathbf{I} , one only needs the names of K candidate classes to perform *zero-shot classification*:

$$\hat{k} = \operatorname{argmax}_k \mathbf{v}^\top \mathbf{t}_k, \quad (1)$$

where $\mathbf{v} = \frac{f(\mathbf{I}; \theta_f)}{\|f(\mathbf{I}; \theta_f)\|_2}$, $\mathbf{t}_k = \frac{g(\mathbf{T}_k; \theta_g)}{\|g(\mathbf{T}_k; \theta_g)\|_2}$; θ_f and θ_g are the frozen parameters of f and g , respectively; \mathbf{T}_k is a text prompt describing the class k , e.g., “a photo of {class $_k$ }”.

3.2. Few-shot classification

Given a set of N labeled samples from each of the K classes, research has been carried out to efficiently adapt CLIP using this set. All existing research in this direction can be gathered in three main avenues (see Fig. 1).

Prompt Tuning. It parameterizes the prompt template, i.e., $\mathbf{T}_k = [\mathbf{w}]_1[\mathbf{w}]_2\dots[\mathbf{w}]_M[\text{class}_k]$, where $[\mathbf{w}]_1, [\mathbf{w}]_2, \dots$, and $[\mathbf{w}]_M$ are learned while keeping f and g frozen. Prompt

tuning adapts CLIP “indirectly” on the classifier side, i.e., the text embeddings are derived from the learned prompts.

Adapters. They learn a multi-layer perceptron (MLP) h with a residual connection α on top of the frozen visual features \mathbf{v} , i.e., $\mathbf{v} := \alpha\mathbf{v} + (1 - \alpha)h(\mathbf{v})$, or on top of the frozen text features \mathbf{t} , i.e., $\mathbf{t} := \alpha\mathbf{t} + (1 - \alpha)h(\mathbf{t})$, or both.

Linear probing. It trains a linear classifier $\mathbf{W} \in \mathbb{R}^{D \times K}$ on top of the frozen visual features, D being the embedding space dimension. The matrix \mathbf{W} can be initialized with text embeddings \mathbf{t}_k as its columns. Since the classifier is directly tuned, linear probing restricts CLIP to K classes after adaptation and cannot be applied in open-class setting.

3.3. CLIP architecture

CLIP adopts a transformer architecture [41] for the text encoder, but the vision encoder may be either a ResNet [13] or a Vision Transformer (ViT) [9]. We detail both architectures below and later elaborate on our unified method applicable to both architectures regardless of their intrinsic differences.

ResNet. CLIP replaces the global average pooling layer in ResNet with an attention pooling layer. The output of the multi-head attention layer is then projected to the shared latent space using a linear layer. Thus, f can be written as $f = f_2 \circ f_1$, where f_1 represents all the layers up to the attention pooling (included), and f_2 represents the linear projection head. Given an image \mathbf{I} :

$$\mathbf{x}_o = f_1(\mathbf{I}), \quad \mathbf{v} = f_2(\mathbf{x}_o) = \mathbf{W}_o^\top \mathbf{x}_o + \mathbf{b}_o, \quad (2)$$

with $\mathbf{x}_o \in \mathbb{R}^{D_o}$ the output of the attention pooling layer, $\mathbf{W}_o \in \mathbb{R}^{D_o \times D}$ the projection matrix and \mathbf{b}_o a bias term.

ViT. The transformer encoder consists of multiple residual attention blocks. Each block has two main components: a multi-head self-attention and a feed-forward neural network (MLP), with residual connections. The output of the last residual attention block is projected to the latent space using a trainable matrix. Thus, f can be written as $f = f_2 \circ f_1$, where f_1 represents all the layers up to the last residual attention block (included), and f_2 represents the projection matrix. Given an image \mathbf{I} :

$$\mathbf{x}_o = f_1(\mathbf{I}), \quad \mathbf{v} = f_2(\mathbf{x}_o) = \mathbf{W}_o^\top \mathbf{x}_o, \quad (3)$$

where no bias term is included, unlike Eq. (2).

Similarly on the text side, the embeddings are projected into the shared latent space using a linear layer.

4. ProLIP

As discussed in Sec. 3.3, CLIP projects both visual and text embeddings into the shared latent space using linear layers. We show that fine-tuning only the projection matrix \mathbf{W}_o in Eq. (2) or Eq. (3) can be a strong alternative to prompt

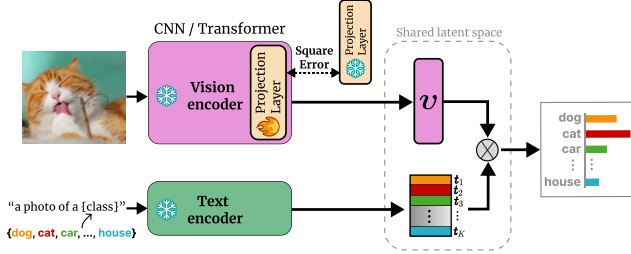


Figure 2. **ProLIP for few-shot adaptation.** Whether the vision encoder is a CNN or a Transformer, ProLIP trains only the layer that projects the visual embeddings into the shared latent space. The text encoder is frozen, and the text embeddings of the K target concepts are used as classification weights. Training with cross-entropy is regularized by a squared error loss ensuring weights of the projection layer to remain close to pretrained ones.

tuning and feature adapters. Specifically, the probability that a sample i belongs to the class k is computed as the Softmax over cosine similarities of image-text embeddings:

$$p_{ik}(\mathbf{W}_o) = \frac{\exp((\mathbf{W}_o^\top \mathbf{x}_{oi} + \mathbf{b}_o)^\top \mathbf{t}_k / \tau)}{\sum_{j=1}^K \exp((\mathbf{W}_o^\top \mathbf{x}_{oi} + \mathbf{b}_o)^\top \mathbf{t}_j / \tau)}, \quad (4)$$

with \mathbf{t}_k being fixed since g is frozen, τ the pretraining temperature parameter, $\mathbf{x}_{oi} = f_1(\mathbf{l}_i)$ the pre-projection embedding of sample i , and \mathbf{b}_o the frozen bias ($\mathbf{0}$ for ViT backbone). The matrix \mathbf{W}_o is learned with gradient descent using a cross-entropy loss $L(\mathbf{W}_o)$:

$$L(\mathbf{W}_o) = -\frac{1}{N} \sum_{i=1}^N \sum_{k=1}^K y_{ik} \log p_{ik}(\mathbf{W}_o), \quad (5)$$

where y_{ik} is the ground truth.

Regularization. CLIP encoders map text and image modalities into a common latent space where strong image-text representation correspondences are established. We argue that unconstrained fine-tuning can lead to forgetting the rich pretraining knowledge that appears through non-trivial zero-shot classification accuracies. Thus, a good fine-tuning strategy should balance pretraining knowledge preservation and adaptation to downstream task. Consequently, to prevent significant drift from the pretraining weights (i.e., knowledge forgetting), we regularize the training with the Frobenius norm of the difference between the pretrained and fine-tuned matrices. The total loss is:

$$\text{Loss} = L(\mathbf{W}_o) + \lambda \|\mathbf{W}_o - \mathbf{W}_o^{(0)}\|_F^2, \quad (6)$$

where $\mathbf{W}_o^{(0)}$ denotes the pretrained value of \mathbf{W}_o . We show later that λ can be chosen as a decreasing function of the number of shots, as overfitting risk increases with less data [12]. The method is illustrated in Fig. 2.

Algorithm 1 PyTorch-like pseudo-code for ProLIP.

```

# target: Ground truth
# lmda: regularization loss weight
# Wo : Pretrained projection matrix
# bo : Pretrained bias term (only ResNet, 0 for ViT)
# xo: output visual embeddings (N*K, Do)
# text_weights: normalized embeddings of classnames (K,D)

# Copy initial weights for use in the regularization loss
Wo_0 = copy.deepcopy(Wo)
# Set embedding projection matrix as trainable weights
Wo.requires_grad = True
bo.requires_grad = False

v = xo @ Wo + bo
v = l2_normalize(v, dim=-1)

#compute the cosine similarity scores
logits = 100. * v @ text_weights.T

#compute regularized loss
SE_loss = nn.MSELoss(reduction='sum')
loss = CE_loss(logits, target) + lmda * SE_loss(Wo, Wo_0)

```

An argument on simplicity and practicality. Algorithm 1 provides a PyTorch-like [31] pseudo-code for ProLIP, showing that it is extremely simple to implement. Also, it can be applied on pre-processed data (i.e., saved pre-projection features), which makes it also extremely fast to train. Practically, we run the inference only one time on the text encoder side to get the classification weights. On the vision encoder side, we save the output embeddings \mathbf{x}_{oi} 's with different augmentation views since backpropagation is limited to the projection matrix.

Despite its extreme simplicity, adapting CLIP using our approach has not been proposed before. Moreover, its architecture-agnostic nature makes it generic and suitable to different multi-modal pretrained networks. Due to intrinsic differences across architectures (e.g., ViT vs. ResNet), finding a unified method to efficiently fine-tune vision-language models based on the pretrained weights is not trivial; ProLIP is the first work to achieve this goal.

5. Experiments

Datasets. Following prior CLIP few-shot learning work, we experimentally test ProLIP on 11 datasets for few-shot classification and base-to-new generalization: ImageNet [8], SUN397 [45], DTD [7], Caltech101 [10], UCF101 [39], Flowers102 [29], StanfordCars [22], FGVAircraft [27], EuroSAT [14], OxfordPets [30] and Food101 [2]. For domain generalization experiments we follow ProGrad [56], using ImageNet as source dataset and testing on ImageNet-V2 [34], ImageNet-Sketch [42], ImageNet-A [16] and ImageNet-R [15] as out-of-distribution datasets. For the cross-dataset transfer experiment, ProLIP is trained on ImageNet and evaluated on the other 10 datasets, similar to ProGrad [56]. For test-time adaptation, we use ImageNet and its out-of-distribution (OOD) variants similarly to TPT [36].

Method	# params	$N = 1$	2	4	8	16
CLIP (0-shot)				58.89		
<i>Prompt tuning</i>						
CoOp [55]	$\bar{K} \times \bar{M} \times \bar{D}_e$	59.62	63.80	67.23	71.30	74.06
PLOT [5]	$P \times K \times M \times D_e$	61.51	65.67	68.39	71.96	74.35
KgCoOp [46]	$K \times M \times D_e$	61.36	63.23	65.73	67.50	69.01
ProGrad [56]	$K \times M \times D_e$	62.46	65.88	68.52	71.82	73.95
<i>Adapters</i>						
CLIP-Adapter [11]	$2(\bar{D}_B \times \bar{D})$	60.32	61.93	65.12	69.20	72.57
Tip-Adapter-F [51]	$N \times K \times D$	61.29	62.94	66.02	69.88	73.82
Tip-Adapter-F* [51]	$N \times K \times D$	63.06	66.47	68.71	71.78	74.37
<i>Linear Probing</i>						
LP [32]	$\bar{K} \times \bar{D}$	36.10	46.99	56.72	64.66	70.56
LP++ [19]	$K \times (D+1)$	63.43	66.20	69.16	72.04	74.42
<i>Model weights</i>						
ProLIP	$D_o \times D$	64.21	67.43	70.58	73.73	76.50

Table 1. **Few-shot classification with few-shot validation.** We report the classification accuracy (%) averaged over 11 datasets and 10 runs, comparing ProLIP to baselines taken from [19]. Note that baselines numbers differ from those reported in the original papers as they used a large validation set to tune hyperparameters. We highlight **best** and **2nd best**. First row provides zero-shot classification for reference. D_e is the dimension of the word embedding space, P the number of prompts in PLOT, M the context length, and D_B the bottleneck dimension of CLIP-Adapter.

Training details. Following prior work we use $N \in \{1, 2, 4, 8, 16\}$ shots as support training set for few-shot classification. For domain generalization and cross-dataset transfer experiments, we use $N=4$ like ProGrad [56]. For base-to-new generalization, we set $N=4$ like ProGrad [56] when using ResNet-50 (RN50) and $N=16$ like MaPLe [21] when using ViT-B/16. Unless otherwise stated, we employ ResNet-50 with CLIP weights as the visual encoder, similarly to the literature. Training runs for 300 epochs on a full-batch of features, taking up to 2s on one Tesla V100.

Baselines. We compare against a variety of existing adaptation strategies that harness only the CLIP model without using external pretrained networks. For *prompt tuning* methods, we report CoOp [55] and its other variants PLOT [5], KgCoOp [46] and ProGrad [56]. For *adapters*, we compare to CLIP-adapter [11] and Tip-adapter [51]. Note that Tip-adapter performance is reported in two settings following [19]: Tip-adapter-F where its two crucial hyperparameters are set to 1 and the validation set is used for early stopping, and Tip-adapter-F* where intensive hyperparameter search is performed to find the best values of the same hyperparameters based on the same validation set. For *linear probing*, we report LP [32] and LP++ [19].

Fair protocol for hyperparameter tuning. Different from the few-shot CLIP literature [51] relying on large validation sets for hyperparameter tuning, authors of LP++ [19] advocate for a few-shot validation set, *i.e.*, using a validation set with as many shots as in the training set. Going one step further, we argue that a truly realistic setting should not

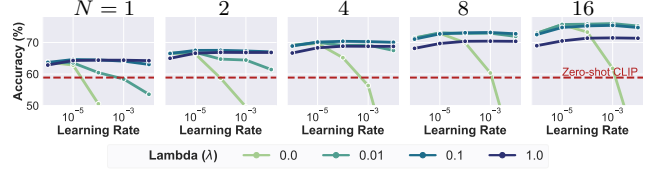


Figure 3. **ProLIP sensitivity to hyperparameter.** Accuracy of ProLIP as function of the hyperparameters (learning rate and regularization weight λ) for $N \in \{1, 2, 4, 8, 16\}$ -shot settings. Each data point is an average over 11 datasets and 10 runs. Detailed numbers for each combination are reported in Tab. 10.

use any validation set as in [38]. For comparison purposes, in Sec. 5.1 we evaluate in the few-shot validation setting, but the core of our evaluation, from Sec. 5.2 onwards, focuses on the *validation-free setting*. Moreover, we evaluate ProLIP on 10 random seeds (*i.e.*, support training sets) for each dataset, as advised by Huang et al. [19].

For Sec. 5.1 only, the learning rate (LR) and regularizer loss weight λ are selected by grid search on the few-shot validation set, with $\text{LR} \in \{10^{-2}, 10^{-3}, 10^{-4}, 10^{-5}, 10^{-6}, 10^{-7}, 10^{-8}\}$ and $\lambda \in \{10, 1, 10^{-1}, 10^{-2}, 10^{-3}, 10^{-4}, 0\}$.

For Sec. 5.2 and following sections, having no access to a validation set, we show that using our regularizer ($\lambda > 0$) prevents severe overfitting, therefore allowing to set a fixed LR over all datasets, and a parametric λ as a decreasing function of the number N of shots.

5.1. Few-shot classification with few-shot validation

Tab. 1 reports the average classification accuracy across 11 datasets and 10 seeds. Per-dataset performances are reported in Appendix A (Tabs. 20 and 21). In all few-shots settings (*i.e.*, $N \in \{1, 2, 4, 8, 16\}$), ProLIP clearly outperforms all the baselines, showing a great potential of the extremely simple approach of fine-tuning the visual embedding linear projector with regularization for adaptation.

Hyperparameters sensitivity. The benefit of the regularization appears by testing ProLIP with different hyperparameters, fixed across datasets. Fig. 3 reports the average accuracy across the same 11 datasets, for 5 different LR values combined either with regularization ($\lambda \in \{10^{-2}, 10^{-1}, 1\}$) or without regularization ($\lambda=0$). For $\lambda=0$, the accuracy drops dramatically for large LR due to overfitting to the few-shot training set, and the subsequent drift from the robust pretrained CLIP representation. On the other hand, using the weight regularizer ($\lambda > 0$) makes ProLIP less prone to overfitting and less sensitive to LR.

This observation is corroborated by the statistics of the hyperparameters found by grid search (*cf.* Appendix B; Fig. 5) showing that the best LR spans a wide range of values. It follows that our regularization alleviates overfitting on the training set, allowing larger LR

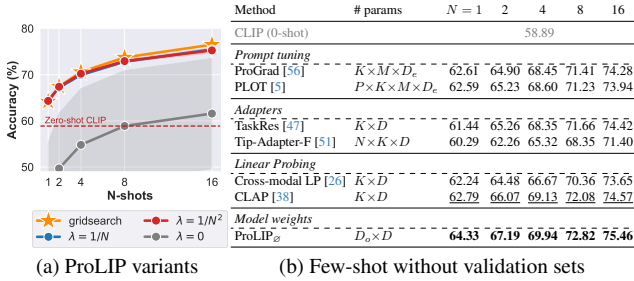


Table 2. **Few-shot classification without validation set.** (a) ProLIP variants with performance averaged over 11 datasets, 10 runs, and 4 learning rates $LR \in \{10^{-5}, 10^{-4}, 10^{-3}, 10^{-2}\}$ to study sensitivity. Note the low variance of the parametric formulations ($\lambda = 1/N$, $\lambda = 1/N^2$) which are also reaching performance of the grid search variant — despite having no access to a validation set. (b) Comparison to validation-free baselines from [38] showing the consistent superiority of ProLIP $_{\emptyset}$. Tab. 1 defines D_e , M & P .

(e.g., 10^{-2}). This important property motivates our investigation of a more realistic setting, where hyperparameters are never tuned: *Having no validation data*.

5.2. Few-shot classification without validation set

An additional merit of ProLIP stems from its lower sensitivity to hyperparameters, as demonstrated in the previous section. It can be observed from Fig. 3 that for lower-shot settings, higher λ values lead to better accuracy, and vice versa. Therefore, we formulate λ as a decreasing function of the number of shots N , reporting in Tab. 2a the average performance over learning rates $LR \in \{10^{-5}, 10^{-4}, 10^{-3}, 10^{-2}\}$. It results that our simple parametric formulations of λ (i.e., $1/N$, $1/N^2$) lead to almost identical, strong and stable results, competing with our state-of-the-art grid search variant, albeit without the need of a validation set. A byproduct of our regularizer is the reduced sensitivity to the learning rate (i.e., low variance as seen in Tab. 2a), whereas removing the regularizer (i.e., $\lambda = 0$) proves to result in dramatically large variance. Detailed numbers for each combination are reported in Tab. 11. Therefore, in Tab. 2b we compare the average across 11 datasets of the validation-free baselines from [38], and the validation-free ProLIP variant, coined as ProLIP $_{\emptyset}$, with $\lambda = 1/N$ and average over the 4 tested learning rates. The reported performance shows a consistent improvement for any N .

5.3. Generalization of few-shot models

Achieving generalization in a few-shot framework is challenging but crucial for evaluating the practical use of few-shot methods. We here explore three aspects of generalization: domain generalization, cross-dataset generalization and base-to-new generalization. Comparison is done only among the few-shot methods; the zero-shot CLIP perfor-

Method	Source										Target													
	ImageNet	Caltech101	OxfordPets	StanfordCars	Flowers102	Food101	FGVCAircraft	SUN397	DTD	Eurosat	UCF101	Average	ImageNet	Caltech101	OxfordPets	StanfordCars	Flowers102	Food101	FGVCAircraft	SUN397	DTD	Eurosat	UCF101	Average
CLIP (0-shot)	60.35	85.84	85.75	55.78	65.98	77.35	17.07	58.85	42.69	36.22	61.80	58.88												
CoOp	61.34	84.48	85.99	54.16	60.10	75.48	14.09	57.48	35.32	26.72	57.56	55.70												
CoCoOp	61.04	84.73	86.42	52.34	61.24	73.79	13.74	55.94	36.60	23.46	57.97	55.21												
Prograd	62.17	88.30	86.43	55.61	62.69	76.76	15.76	60.16	39.48	24.87	58.70	57.36												
ProLIP $_{\emptyset}$	62.55	86.99	84.00	54.19	64.03	74.95	16.99	59.67	41.09	36.55	60.95	58.36												

Table 3. **Cross-dataset generalization.** Training is performed on 4-shot ImageNet (source), except for ‘CLIP’ which is 0-shot. The learned models are evaluated on 10 other datasets (target). Baselines’ scores are average of 3 runs reported from ProGrad [56].

mance is included as reference. For ProLIP $_{\emptyset}$, we systematically use $\lambda = 1/N$ and a fixed LR of 10^{-5} .

Cross-dataset generalization. This generalization setting was addressed in prompt tuning works [54, 56] where OOD datasets not only come from other domains but may also contain different or more fine-grained classes compared to ones in source. Tab. 3 shows the generalization from ImageNet as source dataset (4-shot) to the 10 other datasets. ProLIP $_{\emptyset}$ outperforms ProGrad on 6 out of 11 datasets and on average. However, it is worth noting that zero-shot CLIP remains the strongest baseline in this setting. As argued in CoCoOp [54], ImageNet contains 1000 classes, mainly consisting of objects. Dog breeds are also present, so good generalization (or at most small zero-shot performance drop) to datasets like OxfordPets and Caltech101 is expected. However, for datasets presenting a larger gap (e.g., fine-grained and/or specialized datasets), generalization is expected to be lower. For such datasets, like FGVCAircraft and DTD, ProLIP $_{\emptyset}$ outperforms other adaptation methods, but remains behind zero-shot accuracy. In short, looking at the generalization of ProLIP $_{\emptyset}$ on each of the 10 datasets, our method is overall retaining zero-shot capability the most and showing better cross-dataset transferability.

Domain generalization. In this setting, the set of classes is fixed in both in-domain and OOD datasets. Following ProGrad, we train ProLIP $_{\emptyset}$ on ImageNet (IN) as source dataset (with $N=4$), and assess it on ImageNet-V2 (IN-V2), ImageNet-Sketch (IN-S), ImageNet-A (IN-A) and ImageNet-R (IN-R). Tab. 4 shows that ProLIP $_{\emptyset}$ is on par with or better than other methods on source and especially OOD domains, for both ResNet and ViT CLIP backbones.

Base-to-new generalization. In this setting, we divide all classes into two groups: base and new classes. Training is performed on base classes and testing on both base and new classes. Moreover, the harmonic mean is reported to assess the trade-off. In Tab. 5, we see that ProLIP $_{\emptyset}$ significantly outperforms ProGrad [56] in *total harmonic mean* across 11 datasets. Additionally, ProLIP $_{\emptyset}$ is competitive with MaPLe [21], a method specifically designed for few-shot generalization. For the sake of comparison fairness, we

Method	RN50		RN101		ViT-B/16		ViT-B/32	
	IN	OOD	IN	OOD	IN	OOD	IN	OOD
CLIP (0-shot)	60.34	43.31	61.24	48.71	68.79	59.87	62.00	50.06
LP	41.29	21.19	47.01	28.33	54.70	35.09	46.77	28.81
CoOp	61.34	40.84	63.99	47.48	69.86	58.32	64.74	48.06
CoCoOp	61.04	40.42	63.59	47.34	70.13	58.17	64.63	47.93
Prograd	62.17	42.23	64.98	48.53	70.45	59.05	65.36	49.39
TaskRes	62.61	42.55	65.57	48.19	71.01	59.59	65.99	49.63
Tip-Adapter-F	60.88	41.72	64.85	48.64	70.17	59.04	65.63	49.97
ProLIP $_{\emptyset}$	62.55	43.20	65.11	48.81	70.94	59.97	66.00	49.86

Table 4. **Domain generalization.** 4-shot training on ImageNet (source) and evaluation on OOD variants (IN-V2, IV-S, IN-A, IN-R) with different visual backbones. We report accuracy over source ImageNet (IN) along with the average only over OOD variants to show generalization (‘OOD’). All baselines are reported from ProGrad [56] except for TaskRes and Tip-Adapter-F which we re-implemented.

	Base			New			H														
	CLIP	CoOp	CoCoOp	ProGrad	ProLIP $_{\emptyset}$	CLIP	CoOp	CoCoOp	MaPLe*	MaPLe †	MaPLe ‡	ProLIP $_{\emptyset}$									
(a) ResNet-50	61.72	65.91	63.75	71.96	61.26	66.18	72.23	60.77	66.01	73.29	65.96	69.43	72.31								
(b) ViT-B/16	69.34	74.22	71.70	82.69	63.22	71.66	80.47	71.69	75.83	80.10	73.52	76.67	82.29	74.34	78.11	82.28	75.14	78.55	84.01	73.86	78.61

Table 5. **Base-to-new.** Performance comparison of methods on ResNet-50 and ViT-B/16 architectures across 11 datasets.

report the three variants of MaPLe. MaPLe ‡ trains $9\times$ more parameters than ProLIP (3.55M vs. 0.39M). MaPLe † is on par with ProLIP in the numbers of parameters (0.41M vs. 0.39M). MaPLe* is a shallow version that trains prompts only on the first layer of vision and language branches. Our method is architecture agnostic, while MaPLe in all its versions works only on ViTs and requires backpropagation over the entire vision and text encoders.

Per-dataset performance is reported in Appendix C.

5.4. Analysis and Discussion

Comparison to full and last layer fine-tuning. We compare ProLIP $_{\emptyset}$ with full fine-tuning of the visual backbone. Results in Tab. 6 show that full fine-tuning is far behind ProLIP $_{\emptyset}$, and even degrades zero-shot performance for $N = 1, 2$ and 4-shots. LR is 10^{-5} for these experiments, and ProLIP $_{\emptyset}$ is shown for different λ values (including $\lambda = 0$). These results confirm that full fine-tuning faces a high risk of overfitting especially in low-shot regimes, advocating for PEFT methods like ProLIP.

Moreover, we show the results of fine-tuning the last layer (i.e. the attention pooling layer) of the backbone. For the same LR= 10^{-5} , the performance lags behind ProLIP $_{\emptyset}$, with $8\times$ more trainable parameters. Importantly, we also add results of last-layer fine-tuning when we increase LR to 10^{-4} , showing dramatically decreased performance, espe-

Method	# params	$N = 1$	2	4	8	16
CLIP (0-shot)	-			58.89		
Full Fine-tuning	38.32M	46.09	51.85	58.06	62.22	67.74
Last layer FT (10^{-5})	14.79M	61.26	64.37	67.99	71.58	75.53
Last layer FT (10^{-4})	14.79M	47.47	54.84	62.69	68.98	74.56
ProLIP $_{\emptyset}$ ($\lambda = 0$)	2.10M	62.84	66.35	69.69	72.89	75.65
ProLIP $_{\emptyset}$ ($\lambda = 1/N$)	2.10M	64.28	67.07	69.68	72.57	75.20
ProLIP $_{\emptyset}$ ($\lambda = 1/N^2$)	2.10M	64.28	67.32	70.22	73.10	75.68

Table 6. **Comparison to full fine-tuning.** We report the classification accuracy (%) averaged over 11 datasets, comparing ProLIP $_{\emptyset}$ to full fine-tuning of the vision encoder, and fine-tuning (‘FT’) only the last layer, i.e. the attention pooling layer.

Method	$N = 1$	2	4	8	16
CLIP (0-shot)			58.89		
ProLIP $_{\emptyset}$	64.40	67.28	70.08	72.97	75.57
ProLIP $_{\emptyset}$ + Tip-Adapter-F [51]	64.53	67.47	70.30	73.23	75.89
ProLIP $_{\emptyset}$ + TaskRes [47]	65.01	68.18	71.00	73.78	76.23

Table 7. **Complementarity to other methods.** We report the classification accuracy (%) averaged over 11 datasets and 10 runs. LR is fixed to 10^{-4} for all datasets, and $\lambda = 1/N$.

cially for extremely low-shot setting (e.g., 1-shot).

Complementarity to other methods. We explore whether our method is complementary to others that train different components. Tab. 7 corroborates this complementarity, showing the benefit of combining ProLIP $_{\emptyset}$ with either TaskRes or Tip-Adapter-F. We argue, from the same perspective of logit bias discussed in [40], that each of these methods learns a specific bias on top of zero-shot CLIP, and that these biases contain orthogonal information. For instance, TaskRes learns an element-wise adapter on top of the text embeddings (i.e., the classifier weights), while Tip-Adapter-F learns an adapter initialized with intra-modal similarities (i.e., cache model). ProLIP’s learned bias stems from re-leveraging the pre-projection features to create new combinations adapted to the fixed probe. More details are provided in Appendix F.

Revisiting CLIP-Adapter [11] with ProLIP’s principles. ProLIP fine-tunes a linear transformation of pre-projected features, starting from the zero-shot model and regularizing the weights to stay close to their initial values. We revisit CLIP-Adapter [11] and incorporate ProLIP’s principles by (i) replacing the non-linear MLP with a simple linear transformation, (ii) initializing it with the identity matrix instead of random weights, and (iii) regularizing it during training with a square-error loss. Consequently, this variant of CLIP-Adapter, called Linear Adapter, begins training from the original CLIP weights, similar to ProLIP. Fig. 4 shows that, in the validation-free setting, Linear Adapter significantly outperforms CLIP-Adapter with different values of the residual weight (α), across a wide range of

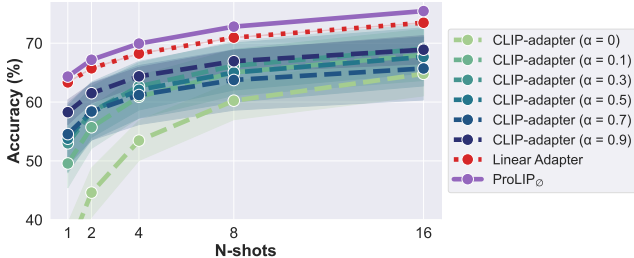


Figure 4. **Improving CLIP-Adapter with ProLIP’s principles** results in the Linear Adapter variant. We report classification accuracy (%) averaged over 11 datasets, 10 runs, and 4 learning rates $LR \in \{10^{-5}, 10^{-4}, 10^{-3}, 10^{-2}\}$ for CLIP-Adapter with different α values, ProLIP_\emptyset and Linear Adapter with $\lambda = 1/N$. Variance is scaled by 60% for readability.

Method	$N = 1$	2	4	8	16
CLIP (0-shot)			58.89		
ProLIP_\emptyset (text)	64.05	66.93	69.71	72.56	75.01
ProLIP_\emptyset (ours)	64.33	67.19	69.94	72.82	75.46

Table 8. **Comparison to fine-tuning the text embedding projection matrix.** We report the classification accuracy (%) averaged over 11 datasets, 10 runs, and 4 learning rates $LR \in \{10^{-5}, 10^{-4}, 10^{-3}, 10^{-2}\}$ where we fine-tune the text projection matrix instead of the visual one, with the same regularization strategy. We call this variant ‘ ProLIP_\emptyset (text)’ and use $\lambda = 1/N$.

$LR (10^{-5}, 10^{-4}, 10^{-3}, 10^{-2})$, while still performs worse than ProLIP_\emptyset . Detailed results for each LR are reported in Tab. 16 (cf. Appendix F). These results reinforce the foundational principles of ProLIP and shed further light on why it is so effective, apart from the perhaps surprising effect of the visual embedding projector.

Can the text embedding projector work? As discussed in Sec. 3.3, CLIP also maps text embeddings to the shared space using a projection matrix. We show here the results of fine-tuning this matrix instead of the visual counterpart, using the same regularization strategy. Tab. 8 shows that this variant is also a strong baseline, though underperforming ProLIP_\emptyset where the visual embedding projection is fine-tuned. Detailed results are reported in Appendix D.

5.5. Extending ProLIP to Test-time Adaptation

In this section, our goal is to show that ProLIP can be applied beyond supervised few-shot CLIP adaptation. Motivated by the risk of “overfitting” the source domain in classic prompt tuning methods [54, 55], Shu et al. [36] pioneered test-time prompt tuning (TPT), aiming to learn adaptive prompts on the fly using a single test image.

TPT background knowledge. TPT aims to learn a context specific to each test image in an unsupervised way. Given an unlabeled test image \mathbf{I}_{test} , the prompt is learned by min-

Method	IN	IN-A	IN-V2	IN-R	IN-S	Average	Avg. OOD
CLIP (0-shot)	60.33	23.79	53.31	60.58	35.46	46.69	43.29
<i>w/o few-shot training on IN</i>							
TPT [36]	60.74	26.67	54.70	59.11	35.09	47.26	43.89
$\text{ProLIP}_{\text{test-time}}$	62.00	33.76	56.03	62.69	37.29	50.35	47.44
<i>w/ 16-shot training on IN</i>							
CoOp [36]	63.33	23.06	55.40	56.60	34.67	46.61	42.43
TPT + CoOp [36]	64.73	30.32	57.83	58.99	35.86	49.55	45.75
ProLIP	64.48	22.75	56.24	59.56	34.80	47.57	43.34
$\text{ProLIP}_{\text{test-time}}$ + ProLIP	66.90	32.96	58.77	61.78	36.97	51.48	47.62

Table 9. **Robustness to natural distribution shifts in test-time adaptation.** Experiments are done with RN50 backbone, without few-shot training on IN (top) and with 16-shot training (bottom).

imizing the average prediction entropy over different augmented views of \mathbf{I}_{test} . Moreover, *confidence selection* filters out the augmented views with high entropy predictions, which might lack important information for classification. More details are provided in Appendix E.

Test-time ProLIP. We do not introduce a new way for CLIP test-time adaptation but simply follow the same experimental setting as TPT (i.e., 1-step entropy minimization of averaged prediction probability distribution, confidence selection), although ProLIP optimizes the projection weight matrix \mathbf{W}_o instead of the prompt as in TPT. We name this ProLIP variant as $\text{ProLIP}_{\text{test-time}}$. Tab. 9 shows that $\text{ProLIP}_{\text{test-time}}$ yields superior results to TPT on ImageNet and natural distribution shifts, while being one order of magnitude faster to train. For direct comparison, we separate methods that perform 16-shot training on ImageNet. Of note, even without few-shot training, $\text{ProLIP}_{\text{test-time}}$ still outperforms CoOp and TPT+CoOp. We further advance $\text{ProLIP}_{\text{test-time}}$ results with 16-shot training.

6. Conclusion

We propose a simple and efficient method for adapting CLIP for few-shot classification by fine-tuning the visual projection matrix, which maps visual embeddings to the multi-modal latent space. Moreover, we show advantages of including a squared error regularizer: it prevents the drift from pretrained weights and improves robustness to hyperparameter choice, thus making our method an appealing and practical approach to few-shot adaptation. Additionally, we provide evidence of the competitiveness of ProLIP in few-shot classification, generalization and test-time adaptation, rendering it a potential general framework for further applications. Finally, we showed the complementarity of ProLIP with other methods and reflect on the practice of using non-linear adapters from our method’s perspective.

Future directions. Our framework can be applied to other foundation models with different modalities, downstream tasks and training objectives [24, 49]. Future research can explore other alternatives for model weights based adaptation, and theoretical investigation on the effect of fine-

tuning the embedding projection matrix.

Acknowledgment. This work was partially funded by French project SIGHT (ANR-20-CE23-0016). It was performed using HPC resources from GENCI- IDRIS (Grants AD011014477R1, AD011012808R3). The authors thank Clément Weinreich for insightful discussion.

Appendix

This document provides details on:

- Per-dataset performance of few-shot classification with few-shot validation in Appendix A, complementing Tab. 1.
- Grid search and hyperparameter sensitivity in Appendix B, as well as Tab. 2a, Tab. 2b and Fig. 3 data.
- Base-to-new generalization in Appendix C.
- Per-LR performance of fine-tuning the text embedding projection matrix in Appendix D.
- Test-time adaptation in Appendix E.
- Analysis and Discussion section (Sec. 5.4) in Appendix F, in particular complementarity and linear adapter. We also provide additional experiments and ablations.
- Training of ProLIP in Appendix G.

A. Details on few-shot classification with few-shot validation

In addition to the average across datasets in Tab. 1, Tabs. 20-21 provide the *per-dataset performance* of all methods, with for each the average accuracy over 10 seeds (i.e., support sets). ProLIP performs particularly well on DTD, UCF101, StanfordCars, FGVCAircraft and EuroSAT. For some specific settings, e.g., 1-shot DTD, 16-shot StanfordCars, 8 and 16-shot FGVCAircraft, the improvements over state-of-the-art are significant. On the other hand, for datasets like OxfordPets and Food101, where the zero-shot performance is already good, ProLIP and other baselines are outperformed by prompt learning methods (e.g., ProGrad). This might be due to the relatively lower number of parameters in the latter, making them less prone to overfitting in very low-shot settings; when the number of shots increases, e.g., 8-16 shots, ProLIP and prompt learning perform on par.

Future research may include the zero-shot accuracy on the few-shot training set in the parametric formulation of the regularization loss weight (i.e., λ). That is, the higher the zero-shot accuracy, the smaller should be the distance between the fine-tuned projection matrix and the pretrained one (i.e., higher λ).

B. ProLIP hyperparameters study

Grid search. Fig. 5 shows the distribution of hyperparameters found by grid search on the few-shot validation set (cf. Tab. 1). We draw two observations:

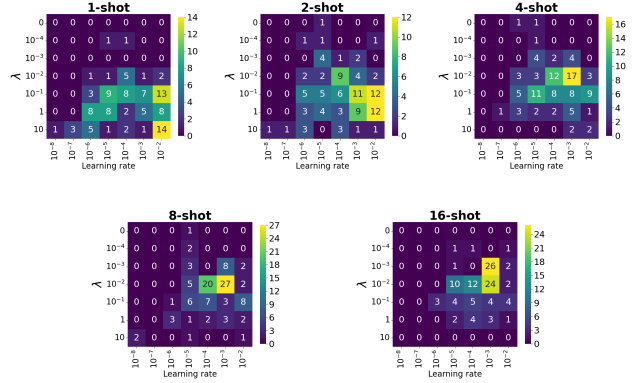


Figure 5. **Hyperparameters selected by grid search.** Learning rates and regularization loss weights λ found with grid search on the few-shot validation set. The distribution of these hyperparameters are shown for each few-shot setting ($N = 1, 2, 4, 8, 16$).

1. The learning rates span a wide range of values, and high values like 10^{-3} and 10^{-2} are selected several times, which would cause severe overfitting when no regularization is used (cf. Tab. 11 and Fig. 3).
2. $\lambda = 0$ is rarely selected, meaning that based on the few-shot validation set, regularized projection matrices generalize better.

Hyperparameter sensitivity. Tab. 10 complements Fig. 3, where ProLIP is trained for different fixed learning rates, with fixed regularization loss weight λ . Looking at the values, we make the following observations:

1. For low learning rates (i.e., 10^{-5} , 10^{-6}), unregularized ProLIP shows good performance for different values of N , demonstrating the effectiveness of simply fine-tuning the visual projection matrix. However, the performance drops significantly when the LR increases.
2. A higher value of λ works better for fewer training shots N , and vice versa. This effect is increasingly visible when the LR increases. Such observation is expected: with less data we need more regularization as overfitting risk is higher, and this is the base for formulating λ as a decreasing function of N (See Tab. 11, which shows the detailed numerical results of Tab. 2a).

C. Details on base-to-new generalization

Metrics details. Previous works [21, 56] calculate the *total harmonic mean* over datasets in two different ways.

To extend Tab. 5, in Tab. 12 we report for each architecture both ways of calculating the *total harmonic means*, renaming them H_{t1} and H_{t2} for disambiguation. It highlights the superiority of our method, regardless of the total harmonic mean used. We also detail the computation below.

Method	$N = 1$	2	4	8	16	
CLIP (0-shot)			58.89			
ProLIP (grid search)	64.21	67.43	70.58	73.73	76.50	
ProLIP, LR= 10^{-6}	$\lambda = 1$	62.85	64.98	66.66	68.13	68.98
	$\lambda = 10^{-1}$	63.69	66.51	68.87	71.07	72.50
	$\lambda = 10^{-2}$	63.73	66.62	69.09	71.42	72.92
	$\lambda = 0$	63.73	66.64	69.12	71.46	72.96
ProLIP, LR= 10^{-5}	$\lambda = 1$	64.28	66.59	68.30	69.67	70.49
	$\lambda = 10^{-1}$	64.60	<u>67.49</u>	70.13	72.71	74.75
	$\lambda = 10^{-2}$	63.54	66.87	70.03	73.06	75.69
	$\lambda = 0$	62.84	66.35	69.69	72.89	75.65
ProLIP, LR= 10^{-4}	$\lambda = 1$	64.40	66.86	68.82	70.37	71.36
	$\lambda = 10^{-1}$	<u>64.48</u>	67.51	<u>70.37</u>	73.08	75.25
	$\lambda = 10^{-2}$	60.45	64.73	69.04	72.85	75.80
	$\lambda = 0$	50.55	58.69	65.18	69.93	73.28
ProLIP, LR= 10^{-3}	$\lambda = 1$	64.39	66.82	68.78	70.42	71.45
	$\lambda = 10^{-1}$	64.08	67.32	70.28	<u>73.17</u>	75.41
	$\lambda = 10^{-2}$	58.42	64.43	69.16	72.94	<u>75.99</u>
	$\lambda = 0$	40.05	49.60	56.35	60.33	61.79
ProLIP, LR= 10^{-2}	$\lambda = 1$	64.25	66.83	68.75	70.36	71.34
	$\lambda = 10^{-1}$	63.04	67.03	70.05	72.75	74.73
	$\lambda = 10^{-2}$	53.58	61.43	67.47	71.92	75.22
	$\lambda = 0$	19.98	24.12	28.03	32.42	35.62

Table 10. **ProLIP sensitivity to hyperparameter choice.** Accuracy of ProLIP to the hyperparameters (learning rate LR and regularization weight λ) for $N \in \{1, 2, 4, 8, 16\}$ -shot settings. Each number is an average over 11 datasets, 10 runs for each.

Method	$N = 1$	2	4	8	16	
CLIP (0-shot)			58.89			
ProLIP $_{\emptyset}$, $\lambda = 1/N$	LR= 10^{-5}	64.28	67.07	69.68	72.57	75.20
	LR= 10^{-4}	64.40	67.28	70.08	72.97	75.57
	LR= 10^{-3}	64.39	67.20	70.01	73.02	75.73
	LR= 10^{-2}	64.25	67.20	69.98	72.70	75.34
	Average	64.33	<u>67.19</u>	<u>69.94</u>	<u>72.82</u>	75.46
ProLIP $_{\emptyset}$, $\lambda = 1/N^2$	LR= 10^{-5}	64.28	67.32	70.22	73.10	75.68
	LR= 10^{-4}	64.40	67.53	70.36	73.08	75.07
	LR= 10^{-3}	64.39	67.40	70.25	73.10	75.80
	LR= 10^{-2}	64.25	67.31	70.02	72.50	74.50
	Average	64.33	67.39	70.21	72.95	<u>75.26</u>
ProLIP $_{\emptyset}$, $\lambda = 0$	LR= 10^{-5}	62.84	66.35	69.69	72.89	75.65
	LR= 10^{-4}	50.55	58.69	65.18	69.93	73.28
	LR= 10^{-3}	40.05	49.60	56.35	60.33	61.79
	LR= 10^{-2}	19.98	24.12	28.03	32.42	35.62
	Average	43.36	49.69	54.81	58.89	61.59

Table 11. **ProLIP $_{\emptyset}$ with a parametric λ .** Accuracy (%) of ProLIP $_{\emptyset}$ with fixed learning rate (LR) and λ as a function of N . For each λ value, we report performance for different LRs and averaged across LRs. Numbers are averages over 11 datasets and 10 runs. We highlight **best** and 2nd best for averages across LRs.

	Base	New	H _{t1}	H _{t2}
CLIP	61.72	65.91	63.64	63.75
CoOp	71.96	61.26	65.58	66.18
CoCoOp	72.23	60.77	65.35	66.01
ProGrad	73.29	65.96	69.06	69.43
ProLIP _∅	75.45	69.43	72.12	72.31

(a) ResNet-50

	Base	New	H _{t1}	H _{t2}
CLIP	69.34	74.22	71.59	71.70
CoOp	82.69	63.22	70.83	71.66
CoCoOp	80.47	71.69	75.44	75.83
MaPLe	82.28	75.14	78.27	78.55
ProLIP _∅	84.01	73.86	78.28	78.61

(b) ViT-B/16

Table 12. **Base-to-new.** Performance comparison of methods on ResNet-50 and ViT-B/16 architectures across 11 datasets with either H_{t1} (equation 7) or H_{t2} (equation 8). Numbers highlight the superiority of our method.

In ProGrad [56], the total harmonic mean over the 11 datasets is computed as *the average harmonic means of individual datasets*. This writes:

$$H_{t1} = \frac{1}{11} \sum_{i=1}^{11} HM_i, \quad (7)$$

$HM_i = 2 \times \frac{\text{acc}_{b_i} \times \text{acc}_{n_i}}{\text{acc}_{b_i} + \text{acc}_{n_i}}$ being the harmonic mean of dataset i . Here, acc_{b_i} and acc_{n_i} denote the accuracy on base and new classes for dataset i , respectively.

Instead in MaPLe [21], the total harmonic mean over the 11 datasets is calculated as *the harmonic mean of average base and average new classes accuracies*:

$$H_{t2} = 2 \times \frac{\text{acc}_b \times \text{acc}_n}{\text{acc}_b + \text{acc}_n}, \quad (8)$$

where $\text{acc}_b = \frac{1}{11} \sum_{i=1}^{11} \text{acc}_{b_i}$ and $\text{acc}_n = \frac{1}{11} \sum_{i=1}^{11} \text{acc}_{n_i}$.

Per-dataset performance. In addition to the cross-datasets performance reported above, we report in Tab. 14 and Tab. 15 the per-dataset accuracy for base and new classes, as well as the harmonic mean metrics.

D. Fine-tuning the text embedding projector

Instead of fine-tuning the visual projection matrix \mathbf{W}_o , we fine-tune its textual counterpart \mathbf{W}_{ot} , with the same strategy adopted in ProLIP_∅. That is, the visual backbone, including \mathbf{W}_o , is frozen. Only \mathbf{W}_{ot} is trained with:

$$\text{Loss} = L(\mathbf{W}_{ot}) + \lambda \|\mathbf{W}_{ot} - \mathbf{W}_{ot}^{(0)}\|_F^2, \quad (9)$$

where λ is set to $\frac{1}{N}$. Tab. 13 complements Tab. 8, showing the performance of this version, coined ‘ProLIP_∅ (text)’, for different values of LR. We note that this baseline is strong, yet still underperforming ProLIP_∅ and exhibiting more sensitivity to the choice of LR.

E. Details on test-time ProLIP

TPT [36] learns a single prompt for each test image using an unsupervised loss function. Given a test image \mathbf{l}_{test} , the image is augmented N_{views} times using a family of random

Method	LR	N = 1	2	4	8	16
CLIP (0-shot)		58.89				
ProLIP _∅ (text)	10 ⁻⁵	64.25	67.10	69.91	72.82	75.34
	10 ⁻⁴	64.13	67.14	70.01	72.80	75.20
	10 ⁻³	63.99	66.74	69.52	72.41	75.00
	10 ⁻²	63.81	66.72	69.39	72.21	74.51

Table 13. **Fine-tuning the text embedding projection matrix.** We report classification accuracy (%) of ‘ProLIP_∅ (text)’ averaged over 11 datasets and 10 runs, using different learning rates (LR).

augmentations \mathcal{A} . Predictions are made for each view, and the training consists of minimizing the entropy of the averaged probability distribution of these predictions:

$$\mathbf{p}^* = \underset{\mathbf{p}}{\text{argmin}} \mathbf{p} - \sum_{i=1}^K \tilde{p}_{\mathbf{p}}(y_i | \mathbf{l}_{\text{test}}) \log \tilde{p}_{\mathbf{p}}(y_i | \mathbf{l}_{\text{test}}), \quad (10)$$

where

$$\tilde{p}_{\mathbf{p}}(y_i | \mathbf{l}_{\text{test}}) = \frac{1}{N_{\text{views}}} \sum_{i=1}^{N_{\text{views}}} p_{\mathbf{p}}(y_i | \mathcal{A}_i(\mathbf{l}_{\text{test}})). \quad (11)$$

In addition, *confidence selection* is used to filter out predictions with high entropy, which are considered as noisy. Self-entropy is computed for each of the N_{views} ; a fixed cut-off percentile ρ keeps only predictions with lower entropy than τ . In Equation 10, $\tilde{p}_{\mathbf{p}}$ becomes:

$$\tilde{p}_{\mathbf{p}}(y | \mathbf{l}_{\text{test}}) = \frac{1}{\rho N} \sum_{i=1}^{N_{\text{views}}} 1_{\{H(p_i) \leq \tau\}} p_{\mathbf{p}}(y | \mathcal{A}_i(\mathbf{l}_{\text{test}})). \quad (12)$$

We apply the same framework (i.e., loss function, confidence selection) with the only difference of minimizing Equation 10 over \mathbf{W}_o instead of the prompt \mathbf{p} . For a fair comparison, we use the same number of steps for training (i.e., 1 step) and the same value of the cutoff percentile $\rho = 0.1$. The learning rate is 10⁻⁴. Note that, measured on ImageNet, ProLIP is ~ 13 times faster than TPT, as the latter requires backpropagation through the whole text encoder, while in our case backpropagation is limited to the visual projection layer and is not applied on the text encoder. We also stress that since we perform only 1 step of training, the regularization loss cannot be used as the first value it takes is 0 (initially the fine-tuned projection matrix is equal to the pre-trained one).

F. Further analysis and discussion

Complementarity to other methods. We showed in Tab. 7 that ProLIP is complementary to other methods that learn different components for few-shot adaptation. Recently, Tang et al. [40] proposed interpreting CLIP few-shot adaptation methods from a unified perspective of logit

	Base	New	H _{t1}	H _{t2}
CLIP	61.72	65.91	63.64	63.75
CoOp	71.96	61.26	65.58	66.18
CoCoOp	72.23	60.77	65.35	66.01
ProGrad	73.29	65.96	69.06	69.43
ProLIP _∅	75.45	69.43	72.12	72.31

(a) Average over 11 datasets.

	Base	New	HM
CLIP	55.55	66.35	60.47
CoOp	61.77	62.51	62.14
CoCoOp	61.68	59.98	60.82
ProGrad	63.01	64.32	63.66
ProLIP _∅	64.61	65.93	65.26

(e) StanfordCars

	Base	New	HM
CLIP	66.45	70.17	68.26
CoOp	71.48	65.57	68.40
CoCoOp	71.88	67.10	69.41
ProGrad	73.71	69.78	71.69
ProLIP _∅	75.20	72.69	73.92

(i) SUN397

	Base	New	HM
CLIP	64.46	59.99	62.14
CoOp	65.49	57.70	61.35
CoCoOp	66.21	58.01	61.84
ProGrad	66.96	60.04	63.23
ProLIP _∅	67.39	62.24	64.71

(b) ImageNet

	Base	New	HM
CLIP	64.10	70.92	67.34
CoOp	89.33	62.77	73.73
CoCoOp	88.07	66.26	75.62
ProGrad	88.19	69.38	77.66
ProLIP _∅	89.42	72.34	79.98

(f) Flowers102

	Base	New	HM
CLIP	49.31	54.35	51.71
CoOp	67.71	43.92	53.28
CoCoOp	63.54	40.78	49.68
ProGrad	66.90	53.06	59.18
ProLIP _∅	71.00	57.09	63.29

(j) DTD

	Base	New	HM
CLIP	90.90	90.72	90.81
CoOp	94.38	87.48	90.80
CoCoOp	94.43	87.81	91.00
ProGrad	94.47	90.84	92.46
ProLIP _∅	95.39	91.15	93.22

(c) Caltech101

	Base	New	HM
CLIP	81.48	82.15	81.81
CoOp	80.40	81.09	80.74
CoCoOp	79.77	77.68	78.71
ProGrad	83.10	83.57	83.33
ProLIP _∅	82.39	84.47	83.42

(g) Food101

	Base	New	HM
CLIP	85.86	93.85	89.68
CoOp	90.31	94.03	92.13
CoCoOp	89.07	91.00	90.02
ProGrad	91.78	94.86	93.29
ProLIP _∅	90.86	93.13	91.98

(d) OxfordPets

	Base	New	HM
CLIP	63.70	67.71	65.64
CoOp	74.59	58.23	65.40
CoCoOp	73.51	59.55	65.80
ProGrad	75.66	65.52	70.23
ProLIP _∅	78.89	71.13	74.81

(h) FGVC Aircraft

	Base	New	HM
CLIP	39.26	43.62	41.33
CoOp	73.53	40.19	51.97
CoCoOp	83.63	40.95	54.98
ProGrad	79.67	49.99	61.43
ProLIP _∅	88.16	66.69	75.94

(k) EuroSAT

	Base	New	HM
CLIP	17.89	25.13	20.90
CoOp	22.53	20.40	21.41
CoCoOp	22.73	19.40	20.93
ProGrad	22.77	24.24	23.48
ProLIP _∅	26.67	26.92	26.79

(l) UCF101

Table 14. **Base-to-new generalization with ResNet-50.** Per-dataset base, new, and harmonic mean accuracy of ProLIP_∅ with $N = 4$ (except ‘CLIP’ which is zero-shot); cf. Tab. 5(a).

	Base	New	H _{t1}	H _{t2}
CLIP	69.34	74.22	71.59	71.70
CoOp	82.69	63.22	70.83	71.66
CoCoOp	80.47	71.69	75.44	75.83
MaPLe	82.28	75.14	78.27	78.55
ProLIP _∅	84.01	73.86	78.28	78.61

(a) Average over 11 datasets.

	Base	New	HM
CLIP	63.37	74.89	68.65
CoOp	78.12	60.40	68.13
CoCoOp	70.49	73.59	72.01
MaPLe	72.94	74.00	73.47
ProLIP _∅	80.08	70.81	75.16

(e) StanfordCars

	Base	New	HM
CLIP	72.43	68.14	70.22
CoOp	76.47	67.88	71.92
CoCoOp	75.98	70.43	73.10
ProGrad	76.66	70.54	73.47
ProLIP _∅	76.62	69.75	73.02

(b) ImageNet

	Base	New	HM
CLIP	72.08	77.80	74.83
CoOp	97.60	59.67	74.06
CoCoOp	94.87	71.75	81.71
ProGrad	95.92	72.46	82.56
ProLIP _∅	96.99	74.30	84.14

(f) Flowers102

	Base	New	HM
CLIP	96.84	94.00	95.40
CoOp	98.00	89.81	93.73
CoCoOp	97.96	93.81	95.84
ProGrad	97.74	94.36	96.02
ProLIP _∅	98.50	94.51	96.46

(c) Caltech101

	Base	New	HM
CLIP	27.19	36.29	31.09
CoOp	40.44	22.30	28.75
CoCoOp	33.41	23.71	27.74
ProGrad	37.44	35.61	36.50
ProLIP _∅	43.15	33.86	37.94

(d) OxfordPets

	Base	New	HM
CLIP	53.24	59.90	56.37
CoOp	79.44	41.18	54.24
CoCoOp	77.01	56.00	64.85
ProGrad	80.36	59.18	68.16
ProLIP _∅	82.13	57.15	67.40

(j) DTD

	Base	New	HM
CLIP	92.19	91.22	90.66
CoOp	88.33	82.26	85.19
CoCoOp	90.70	91.29	90.99
ProGrad	90.71	92.05	91.38
ProLIP _∅	90.31	90.93	90.62

(g) Food101

	Base	New	HM
CLIP	70.53	77.50	73.85
CoOp	84.69	56.05	67.46
CoCoOp	82.33	73.45	77.64
ProGrad	83.00	78.66	80.77
ProLIP _∅	86.64	80.67	83.55

(h) FGVC Aircraft

	Base	New	HM
CLIP	56.48	64.05	60.03
CoOp	92.19	54.74	68.69
CoCoOp	87.49	60.04	71.21
ProGrad	94.07	73.23	82.35
ProLIP _∅	92.67	66.07	77.14

(k) EuroSAT

	Base	New	HM
CLIP	70.53	77.50	73.85
CoOp	84.69	56.05	67.46
CoCoOp	82.33	73.45	77.64
ProGrad	83.00	78.66	80.77
ProLIP _∅	86.64	80.67	83.55

(l) UCF101

Table 15. **Base-to-new generalization with ViT-B/16.** Per-dataset base, new, and harmonic mean accuracy of ProLIP_∅ with $N = 16$ (except ‘CLIP’ which is zero-shot); cf. Tab. 5(b).

bias. That is, every method learns a bias on top of the zero-shot CLIP logits. We detail here the bias learned by each the two methods ProLIP was shown to be complementary to: TaskRes and Tip-Adapter-F, as well as the bias learned by ProLIP. TaskRes learns an element-wise adapter on top of \mathbf{t} , the text-based frozen classifier. It writes:

$$\text{Logits}_{\text{TaskRes}} = \mathbf{v}^\top(\mathbf{t} + \alpha \mathbf{r}) = \underbrace{\mathbf{v}^\top \mathbf{t}}_{\text{zero-shot logits}} + \alpha \mathbf{v}^\top \mathbf{r}. \quad (13)$$

The bias learned by TaskRes is thus a new linear probe trained on top of frozen visual features \mathbf{v} .

Tip-Adapter-F builds a cache model from the training features $\mathbf{F}_{\text{train}}$ and their labels $\mathbf{L}_{\text{train}}$. It writes:

$$\text{Logits}_{\text{Tip-Adapter-F}} = \underbrace{\mathbf{v}^\top \mathbf{t}}_{\text{zero-shot logits}} + \alpha \phi(\mathbf{v}^\top \mathbf{F}_{\text{train}}^\top) \mathbf{L}_{\text{train}}. \quad (14)$$

$\mathbf{F}_{\text{train}}$ is fine-tuned, thus the bias is based on intra-modal similarity measures (i.e., similarities in the visual space).

For ProLIP, we fine-tune the projection matrix \mathbf{W}_o . Omitting b_o for simplicity, the logits can be written as:

$$\text{Logits}_{\text{ProLIP}} = \mathbf{x}_o^\top \mathbf{W}_o \mathbf{t} = \underbrace{\mathbf{x}_o^\top \mathbf{W}_o^{(0)} \mathbf{t}}_{\text{zero-shot logits}} + \mathbf{x}_o^\top \mathbf{B} \mathbf{t}. \quad (15)$$

That is, fine-tuning \mathbf{W}_o is equivalent to learning a matrix \mathbf{B} , initialized with $\mathbf{0}_{D_o \times D}$. Thus, the bias learned by ProLIP is a linear combination of the pre-projected features, trained to match the fixed text-based probe \mathbf{t} . In short, each of the three methods learn a different bias, and we hypothesize that the results of Tab. 7 reflect that these biases contain orthogonal knowledge learned during few-shot adaptation.

It is worth noting that we fixed the LR to 10^{-4} for all the datasets in these experiments. While the complementarity was shown for fixed hyperparameters across all datasets, ($\alpha = \beta = 1$ for Tip-Adapter-F and $\alpha = 0.1$ for TaskRes), increasing the LR to 10^{-2} leads to overfitting since the biases of TaskRes and Tip-Adapter-F are not regularized, which highlights again the advantage of ProLIP in stability across LRs.

Revisiting CLIP-Adapter [11] with ProLIP’s principles. When using our proposed linear adapter, the logits write:

$$\text{Logits}_{\text{Linear adapter}} = \mathbf{v}^\top \mathbf{W} \mathbf{t}. \quad (16)$$

We fine-tune the matrix \mathbf{W} , initialized with identity \mathbf{I} , using a cross entropy loss and the regularizer $\frac{1}{N} \|\mathbf{W} - \mathbf{I}\|_F^2$, inspired by ProLIP.

Tab. 16 reports detailed results of CLIP-Adapter when varying its residual weight (α) and the learning rate. Not only are the averaged results significantly worse than those

Method		$N = 1$	2	4	8	16	Average
$\alpha = 0$	LR= 10^{-5}	17.92	30.80	44.39	55.41	63.02	42.31
	LR= 10^{-4}	39.17	50.45	59.91	66.78	71.74	57.61
	LR= 10^{-3}	41.79	51.78	60.04	66.41	71.14	58.23
	LR= 10^{-2}	39.36	45.45	49.47	52.34	53.28	47.98
	Average	34.56	44.62	53.45	60.24	64.80	51.53
$\alpha = 0.1$	LR= 10^{-5}	57.65	62.21	66.46	70.30	73.12	65.95
	LR= 10^{-4}	57.40	62.26	66.84	70.97	74.39	66.37
	LR= 10^{-3}	44.81	53.50	61.25	67.13	71.49	59.64
	LR= 10^{-2}	38.42	44.90	49.05	51.76	53.07	47.44
	Average	49.57	55.72	60.90	65.04	68.02	59.85
$\alpha = 0.3$	LR= 10^{-5}	63.39	66.62	69.39	71.88	73.69	68.99
	LR= 10^{-4}	60.26	64.28	68.23	71.96	75.12	67.97
	LR= 10^{-3}	50.77	58.05	63.86	68.77	72.74	62.84
	LR= 10^{-2}	37.55	44.37	49.22	52.07	54.69	47.58
	Average	52.99	58.33	62.68	66.17	69.06	61.85
$\alpha = 0.5$	LR= 10^{-5}	63.79	66.61	68.72	70.40	71.48	68.20
	LR= 10^{-4}	60.78	64.75	68.48	72.03	74.94	68.20
	LR= 10^{-3}	55.47	60.73	65.62	69.90	73.54	65.05
	LR= 10^{-2}	35.07	41.79	45.50	47.73	50.72	44.16
	Average	53.78	58.47	62.08	65.02	67.67	61.40
$\alpha = 0.7$	LR= 10^{-5}	63.18	64.96	66.01	66.57	66.88	65.52
	LR= 10^{-4}	61.32	65.19	68.69	71.75	74.02	68.19
	LR= 10^{-3}	56.98	61.63	66.15	70.41	74.05	65.84
	LR= 10^{-2}	36.73	41.80	43.91	46.28	47.87	43.32
	Average	54.55	58.40	61.19	63.75	65.71	60.72
$\alpha = 0.9$	LR= 10^{-5}	60.74	60.99	61.04	61.12	61.13	61.00
	LR= 10^{-4}	62.42	65.40	67.38	68.69	69.40	66.66
	LR= 10^{-3}	58.55	63.13	67.47	71.23	74.14	66.90
	LR= 10^{-2}	51.42	56.48	61.59	66.71	70.91	61.42
	Average	58.28	61.50	64.37	66.94	68.90	64.00
Linear Adapter, $\lambda = 1/N$	LR= 10^{-5}	63.23	65.56	68.08	70.90	73.44	68.24
	LR= 10^{-4}	63.41	65.80	68.27	70.91	73.35	68.35
	LR= 10^{-3}	63.38	65.82	68.30	70.99	73.55	68.41
	LR= 10^{-2}	63.35	65.78	68.29	70.99	73.57	68.40
	Average	63.34	65.74	68.24	70.95	73.48	68.35
ProLIP $_{\emptyset}$, $\lambda = 1/N$	LR= 10^{-5}	64.28	67.07	69.68	72.57	75.20	69.76
	LR= 10^{-4}	64.40	67.28	70.08	72.97	75.57	70.06
	LR= 10^{-3}	64.39	67.20	70.01	73.02	75.73	70.07
	LR= 10^{-2}	64.25	67.20	69.98	72.70	75.34	69.89
	Average	64.33	67.19	69.94	72.82	75.46	69.95

Table 16. **Improving CLIP-Adapter with ProLIP’s principles** results in the Linear Adapter variant. We report classification accuracy (%) averaged over 11 datasets, 10 runs, and 4 learning rates $\text{LR} \in \{10^{-5}, 10^{-4}, 10^{-3}, 10^{-2}\}$ for CLIP-Adapter with different α values, ProLIP $_{\emptyset}$ and Linear Adapter with $\lambda = 1/N$.

of the Linear Adapter variant and ProLIP $_{\emptyset}$, but CLIP-Adapter also exhibits high variance, especially in low-shot settings. Incorporating the ProLIP’s principles, Linear Adapter consistently improves performance while being much more stable. Our ProLIP $_{\emptyset}$ still achieves the best results.

Number of augmented views. Following the literature [19, 51], we apply RandomResizedCrop and RandomHorizontalFlip augmentations during training. As mentioned earlier, ProLIP can be applied on pre-computed visual embeddings (before the projection layer). We ablate the number of views in which the features are saved. Fig. 6 shows that average accuracy over 11 datasets increases with more views. Interestingly, ~ 10 views are sufficient to get results close to those with 300 views. In contrast, Lin et al. [26] showed that the gain saturates after more than two views for their cross-modal linear probe.

Visualization. We use UMAP to visualize EuroSAT test

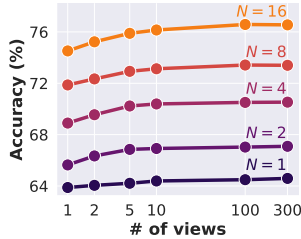


Figure 6. **Effect of augmented views.** Ablation of ProLIP using varying number of views and shots.

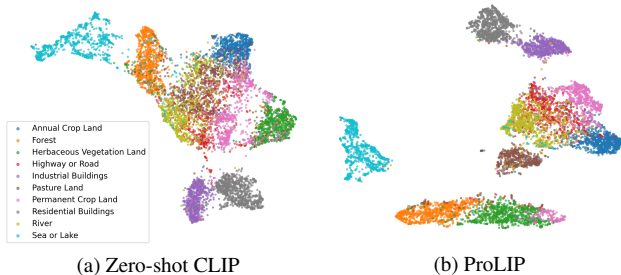


Figure 7. **Ablation and UMAP Visualization.** (a) and (b) UMAP of Zero-shot CLIP vs. ProLIP on EuroSAT, showing that some classes (e.g., ‘Pasture Land’, ‘Permanent Crop Land’, ‘Sea or Lake’, etc.) are better clustered with our method.

set feature manifolds, before and after 16-shot training (i.e., zero-shot vs. ProLIP). The results are illustrated in Figs. 7a and 7b. We observe that the features are generally better clustered for ProLIP. Confusing categories like *Highway or Road*, *Permanent Crop Land* and *Pasture Land* exhibit remarkably better separation for our few-shot adapted model compared to zero-shot. This visualization hints that ProLIP learns better feature manifolds in the few-shot classification setting.

More few-shot settings & Full data training. Training on 32 shots, ProLIP_∅ yields 77.79% average accuracy over 11 datasets and 10 seeds, better than lower-shot results (cf. Tab. 2b). Using full data for training, ProLIP_∅ improves to 81.03% compared to 79.97% for TaskRes. Of note, Tip-adapter-F trains $N_{\text{data}} \times D$ parameters, thus 1.3B parameters for full ImageNet, which is not feasible. This also highlights the benefit of ProLIP for which the number of trainable parameters is not a function of the dataset size.

Effect of temperature. In all the experiments of the paper, we use the pretrained temperature value $\text{temp} = 1/\tau = 100$ (cf. Eq. (4)). Here we ablate this choice and show in Tab. 17 the performance of ProLIP_∅ for $\text{temp} = 50$ and $\text{temp} = 150$. We observe that the performance is not highly affected, and that $\text{temp} = 50$ even out-

temp	$N = 1$	2	4	8	16
50	64.47	67.37	70.25	73.13	75.72
100	64.40	67.28	70.08	72.97	75.57
150	64.15	67.03	69.85	72.70	75.24

Table 17. **Effect of temperature (temp).** We report classification accuracy (%) of ProLIP_∅ averaged over 11 datasets and 10 runs for different temperature values. $\text{LR} = 10^{-4}$ and $\lambda = 1/N$ for all datasets.

performs the pretrained value. Studying in depth the effect of this parameter is left for future research.

G. ProLIP training details

The text encoder is fully frozen during training of ProLIP. The templates are similar to previous works [19, 51] for fair comparison, and are detailed in Tab. 18 for each dataset.

Dataset	Template
Caltech101	“a photo of a {class}.”
StanfordCars	“a photo of a {class}.”
SUN397	“a photo of a {class}.”
DTD	“{class} texture.”
Eurosat	“a centered satellite photo of {class}.”
FGVCAircraft	“a photo of a {class}, a type of aircraft.”
Food101	“a photo of {class}, a type of food.”
Flowers102	“a photo of a {class}, a type of flower.”
OxfordPets	“a photo of a {class}, a type of pet.”
UCF101	“a photo of a person doing {class}.”
ImageNet	Ensemble of 7 templates:
ImageNet-A	{“itap of a {class}.”, “a bad photo of the {class}.”,
ImageNet-V2	“a origami {.”, “a photo of the large {class}.”,
ImageNet-R	“a {class} in a video game.”, “art of the {class}.”,
ImageNet-Sketch	“a photo of the small {class}.”}

Table 18. **Dataset-specific templates.** Following the literature, all but ImageNet dataset and its variants use a single template.

For training, only the weight matrix W_o in Eq. (2) and Eq. (3) is fine-tuned. Note that for ResNets, a bias term b_o exists while for ViTs no bias is added in pretraining. We stress that fine-tuning also the bias term for ResNets does not change the results, as most of the parameters as concentrated in the weight matrix. In detail for ResNet-50, $W_o \in \mathbb{R}^{D_o \times D}$, where $D_o = 2048$ and $D = 1024$, this makes a total of $\sim 2\text{M}$ parameters, while $b_o \in \mathbb{R}^D$ has only 1024 parameters. Tab. 19 shows the number of trainable parameters in ProLIP for different backbones.

Backbone	$D_o \times D$	Parameters in W_o
ResNet-50	2048×1024	2.097M
ResNet-101	2048×512	1.049M
ViT-B/32	768×512	0.393M
ViT-B/16	768×512	0.393M

Table 19. **Number of trainable parameters per backbone.** It is the number of elements in the projection matrix $W_o \in \mathbb{R}^{D_o \times D}$.

References

- [1] Christopher M Bishop and Nasser M Nasrabadi. *Pattern recognition and machine learning*. Springer, 2006. 3
- [2] Lukas Bossard, Matthieu Guillaumin, and Luc Van Gool. Food-101—mining discriminative components with random forests. In *ECCV*, 2014. 4
- [3] Tom Brown, Benjamin Mann, Nick Ryder, Melanie Subbiah, Jared D Kaplan, Prafulla Dhariwal, Arvind Neelakantan, Pranav Shyam, Girish Sastry, Amanda Askell, et al. Language models are few-shot learners. In *NeurIPS*, 2020. 1, 3
- [4] Mathilde Caron, Hugo Touvron, Ishan Misra, Hervé Jégou, Julien Mairal, Piotr Bojanowski, and Armand Joulin. Emerging properties in self-supervised vision transformers. In *ICCV*, 2021. 3
- [5] Guangyi Chen, Weiran Yao, Xiangchen Song, Xinyue Li, Yongming Rao, and Kun Zhang. PLOT: Prompt learning with optimal transport for vision-language models. In *ICLR*, 2023. 1, 2, 5, 6, 17
- [6] Xinlei Chen, Saining Xie, and Kaiming He. An empirical study of training self-supervised vision transformers. In *ICCV*, 2021. 3
- [7] Mircea Cimpoi, Subhansu Maji, Iasonas Kokkinos, Sammy Mohamed, and Andrea Vedaldi. Describing textures in the wild. In *CVPR*, 2014. 4
- [8] Jia Deng, Wei Dong, Richard Socher, Li-Jia Li, Kai Li, and Li Fei-Fei. Imagenet: A large-scale hierarchical image database. In *CVPR*, 2009. 4
- [9] Alexey Dosovitskiy, Lucas Beyer, Alexander Kolesnikov, Dirk Weissenborn, Xiaohua Zhai, Thomas Unterthiner, Mostafa Dehghani, Matthias Minderer, Georg Heigold, Sylvain Gelly, Jakob Uszkoreit, and Neil Houlsby. An image is worth 16x16 words: Transformers for image recognition at scale. In *ICLR*, 2021. 3
- [10] Li Fei-Fei, Rob Fergus, and Pietro Perona. Learning generative visual models from few training examples: An incremental bayesian approach tested on 101 object categories. In *CVPR Workshops*, 2004. 4
- [11] Peng Gao, Shijie Geng, Renrui Zhang, Teli Ma, Rongyao Fang, Yongfeng Zhang, Hongsheng Li, and Yu Qiao. Clip-adapter: Better vision-language models with feature adapters. *IJCV*, 2024. 1, 2, 3, 5, 7, 13, 17
- [12] Trevor Hastie, Robert Tibshirani, Jerome H Friedman, and Jerome H Friedman. *The elements of statistical learning: data mining, inference, and prediction*. Taylor & Francis, 2009. 4
- [13] Kaiming He, Xiangyu Zhang, Shaoqing Ren, and Jian Sun. Deep residual learning for image recognition. In *CVPR*, 2016. 3
- [14] Patrick Helber, Benjamin Bischke, Andreas Dengel, and Damian Borth. Eurosat: A novel dataset and deep learning benchmark for land use and land cover classification. *IEEE Journal of Selected Topics in Applied Earth Observations and Remote Sensing*, 2019. 1, 4
- [15] Dan Hendrycks, Steven Basart, Norman Mu, Saurav Kadavath, Frank Wang, Evan Dorundo, Rahul Desai, Tyler Zhu, Samyak Parajuli, Mike Guo, et al. The many faces of robustness: A critical analysis of out-of-distribution generalization. In *ICCV*, 2021. 4
- [16] Dan Hendrycks, Kevin Zhao, Steven Basart, Jacob Steinhardt, and Dawn Song. Natural adversarial examples. In *CVPR*, 2021. 4
- [17] Neil Houlsby, Andrei Giurgiu, Stanislaw Jastrzebski, Bruna Morrone, Quentin De Laroussilhe, Andrea Gesmundo, Mona Attariyan, and Sylvain Gelly. Parameter-efficient transfer learning for nlp. In *ICML*, 2019. 2
- [18] Edward J Hu, Yelong Shen, Phillip Wallis, Zeyuan Allen-Zhu, Yuanzhi Li, Shean Wang, Lu Wang, and Weizhu Chen. Lora: Low-rank adaptation of large language models. In *ICLR*, 2022. 2
- [19] Yunshi Huang, Fereshteh Shakeri, Jose Dolz, Malik Boudiaf, Houda Bahig, and Ismail Ben Ayed. LP++: A surprisingly strong linear probe for few-shot clip. In *CVPR*, 2024. 1, 2, 3, 5, 13, 14, 17
- [20] Menglin Jia, Luming Tang, Bor-Chun Chen, Claire Cardie, Serge Belongie, Bharath Hariharan, and Ser-Nam Lim. Visual prompt tuning. In *ECCV*, 2022. 2
- [21] Muhammad Uzair Khattak, Hanoona Rasheed, Muhammad Maaz, Salman Khan, and Fahad Shahbaz Khan. Maple: Multi-modal prompt learning. In *CVPR*, 2023. 2, 3, 5, 6, 9, 11
- [22] Jonathan Krause, Michael Stark, Jia Deng, and Li Fei-Fei. 3d object representations for fine-grained categorization. In *ICCV Workshops*, 2013. 4
- [23] Ananya Kumar, Aditi Raghunathan, Robbie Jones, Tengyu Ma, and Percy Liang. Fine-tuning can distort pretrained features and underperform out-of-distribution. In *ICLR*, 2022. 1, 2
- [24] Liunian Harold Li, Pengchuan Zhang, Haotian Zhang, Jianwei Yang, Chunyuan Li, Yiwu Zhong, Lijuan Wang, Lu Yuan, Lei Zhang, Jenq-Neng Hwang, et al. Grounded language-image pre-training. In *CVPR*, 2022. 8
- [25] Xiang Lisa Li and Percy Liang. Prefix-tuning: Optimizing continuous prompts for generation. *ACL*, 2021. 2
- [26] Zhiqiu Lin, Samuel Yu, Zhiyi Kuang, Deepak Pathak, and Deva Ramanan. Multimodality helps unimodality: Cross-modal few-shot learning with multimodal models. In *CVPR*, 2023. 2, 3, 6, 13
- [27] Subhansu Maji, Esa Rahtu, Juho Kannala, Matthew Blaschko, and Andrea Vedaldi. Fine-grained visual classification of aircraft. *arXiv*, 2013. 1, 4
- [28] Sachit Menon and Carl Vondrick. Visual classification via description from large language models. In *ICLR*, 2023. 1
- [29] Maria-Elena Nilsback and Andrew Zisserman. Automated flower classification over a large number of classes. In *ICVGIP*, 2008. 4
- [30] Omkar M Parkhi, Andrea Vedaldi, Andrew Zisserman, and CV Jawahar. Cats and dogs. In *CVPR*, 2012. 4
- [31] Adam Paszke, Sam Gross, Francisco Massa, Adam Lerer, James Bradbury, Gregory Chanan, Trevor Killeen, Zeming Lin, Natalia Gimelshein, Luca Antiga, et al. Pytorch: An imperative style, high-performance deep learning library. In *NeurIPS*, 2019. 4

- [32] Alec Radford, Jong Wook Kim, Chris Hallacy, Aditya Ramesh, Gabriel Goh, Sandhini Agarwal, Girish Sastry, Amanda Askell, Pamela Mishkin, Jack Clark, et al. Learning transferable visual models from natural language supervision. In *ICML*, 2021. 1, 2, 5, 17
- [33] Aditya Ramesh, Mikhail Pavlov, Gabriel Goh, Scott Gray, Chelsea Voss, Alec Radford, Mark Chen, and Ilya Sutskever. Zero-shot text-to-image generation. In *ICML*, 2021. 3
- [34] Benjamin Recht, Rebecca Roelofs, Ludwig Schmidt, and Vaishal Shankar. Do imagenet classifiers generalize to imagenet? In *ICML*, 2019. 4
- [35] Andreas Rücklé, Gregor Geigle, Max Glockner, Tilman Beck, Jonas Pfeiffer, Nils Reimers, and Iryna Gurevych. Adapterdrop: On the efficiency of adapters in transformers. In *EMNLP*, 2021. 2
- [36] Manli Shu, Weili Nie, De-An Huang, Zhiding Yu, Tom Goldstein, Anima Anandkumar, and Chaowei Xiao. Test-time prompt tuning for zero-shot generalization in vision-language models. In *NeurIPS*, 2022. 4, 8, 11
- [37] Yang Shu, Xingzhuo Guo, Jialong Wu, Ximei Wang, Jianmin Wang, and Mingsheng Long. Clipood: Generalizing clip to out-of-distributions. In *ICML*, 2023. 3
- [38] Julio Silva-Rodriguez, Sina Hajimiri, Ismail Ben Ayed, and Jose Dolz. A closer look at the few-shot adaptation of large vision-language models. In *CVPR*, 2024. 1, 2, 3, 5, 6
- [39] K Soomro. Ucf101: A dataset of 101 human actions classes from videos in the wild. *arXiv*, 2012. 4
- [40] Yuwei Tang, Zhenyi Lin, Qilong Wang, Pengfei Zhu, and Qinghua Hu. Amu-tuning: Effective logit bias for clip-based few-shot learning. In *CVPR*, 2024. 3, 7, 11
- [41] Ashish Vaswani, Noam Shazeer, Niki Parmar, Jakob Uszkoreit, Llion Jones, Aidan N Gomez, Lukasz Kaiser, and Illia Polosukhin. Attention is all you need. In *NeurIPS*, 2017. 3
- [42] Haohan Wang, Songwei Ge, Zachary Lipton, and Eric P Xing. Learning robust global representations by penalizing local predictive power. In *NeurIPS*, 2019. 4
- [43] Zhengbo Wang, Jian Liang, Lijun Sheng, Ran He, Zilei Wang, and Tieniu Tan. A hard-to-beat baseline for training-free CLIP-based adaptation. In *ICLR*, 2024. 3
- [44] Zhixiang Wei, Lin Chen, Yi Jin, Xiaoxiao Ma, Tianle Liu, Pengyang Ling, Ben Wang, Huaian Chen, and Jinjin Zheng. Stronger fewer & superior: Harnessing vision foundation models for domain generalized semantic segmentation. In *CVPR*, 2024. 2
- [45] Jianxiong Xiao, James Hays, Krista A Ehinger, Aude Oliva, and Antonio Torralba. Sun database: Large-scale scene recognition from abbey to zoo. In *CVPR*, 2010. 4
- [46] Hantao Yao, Rui Zhang, and Changsheng Xu. Visual-language prompt tuning with knowledge-guided context optimization. In *CVPR*, 2023. 5, 17
- [47] Tao Yu, Zhihe Lu, Xin Jin, Zhibo Chen, and Xinchao Wang. Task residual for tuning vision-language models. In *CVPR*, 2023. 3, 6, 7
- [48] Elad Ben Zaken, Shauli Ravfogel, and Yoav Goldberg. Bitfit: Simple parameter-efficient fine-tuning for transformer-based masked language-models. In *ACL*, 2022. 2
- [49] Xiaohua Zhai, Basil Mustafa, Alexander Kolesnikov, and Lucas Beyer. Sigmoid loss for language image pre-training. In *ICCV*, 2023. 8
- [50] Jeffrey O Zhang, Alexander Sax, Amir Zamir, Leonidas Guibas, and Jitendra Malik. Side-tuning: a baseline for network adaptation via additive side networks. In *ECCV*, 2020. 2
- [51] Renrui Zhang, Wei Zhang, Rongyao Fang, Peng Gao, Kun-chang Li, Jifeng Dai, Yu Qiao, and Hongsheng Li. Tip-adapter: Training-free adaption of clip for few-shot classification. In *ECCV*, 2022. 1, 2, 3, 5, 6, 7, 13, 14, 17
- [52] Renrui Zhang, Xiangfei Hu, Bohao Li, Siyuan Huang, Han-qi Deng, Yu Qiao, Peng Gao, and Hongsheng Li. Prompt, generate, then cache: Cascade of foundation models makes strong few-shot learners. In *CVPR*, 2023. 3
- [53] Zexuan Zhong, Dan Friedman, and Danqi Chen. Factual probing is [mask]: Learning vs. learning to recall. *ACL*, 2021. 2
- [54] Kaiyang Zhou, Jingkang Yang, Chen Change Loy, and Ziwei Liu. Conditional prompt learning for vision-language models. In *CVPR*, 2022. 1, 2, 6, 8
- [55] Kaiyang Zhou, Jingkang Yang, Chen Change Loy, and Ziwei Liu. Learning to prompt for vision-language models. *IJCV*, 2022. 2, 5, 8, 17
- [56] Beier Zhu, Yulei Niu, Yucheng Han, Yue Wu, and Hanwang Zhang. Prompt-aligned gradient for prompt tuning. In *ICCV*, 2023. 1, 2, 4, 5, 6, 7, 9, 11, 17
- [57] Xiangyang Zhu, Renrui Zhang, Bowei He, Aojun Zhou, Dong Wang, Bin Zhao, and Peng Gao. Not all features matter: Enhancing few-shot clip with adaptive prior refinement. In *ICCV*, 2023. 3

Dataset	Method	$N = 1$	2	4	8	16
<i>ImageNet</i>	CLIP (0-shot)			60.35		
	CoOp [55]	61.19	61.58	62.22	62.87	63.70
	PLOT [5]	60.46	60.73	61.79	62.48	63.08
	KgCoOp [46]	60.90	61.44	62.00	62.20	62.43
	ProGrad [56]	61.58	62.14	62.59	63.04	63.54
	CLIP-Adapter [11]	59.82	59.94	59.97	59.98	61.31
	Tip-Adapter-F [51]	60.59	61.42	62.12	63.41	65.06
	Tip-Adapter-F* [51]	60.98	61.23	61.72	62.84	64.03
	Standard LP [32]	22.21	31.96	41.48	49.49	56.04
	LP++ [19]	61.18	61.56	62.55	63.76	64.73
ProLIP	61.28	61.79	62.38	63.30	64.31	
<i>SUN397</i>	CLIP (0-shot)			58.85		
	CoOp [55]	61.79	63.32	65.79	67.89	70.15
	PLOT [5]	62.53	63.87	65.85	67.83	69.90
	KgCoOp [46]	62.91	64.38	66.06	66.66	67.68
	ProGrad [56]	62.79	64.12	66.32	68.33	70.18
	CLIP-Adapter [11]	60.78	61.79	63.84	66.26	67.66
	Tip-Adapter-F [51]	61.02	62.15	63.86	67.25	70.94
	Tip-Adapter-F* [51]	62.58	63.79	65.49	67.43	69.25
	Standard LP [32]	32.56	43.77	54.49	61.83	67.03
	LP++ [19]	62.47	64.65	67.28	69.34	71.23
ProLIP	63.44	65.16	67.39	69.31	71.31	
<i>DTD</i>	CLIP (0-shot)			42.69		
	CoOp [55]	42.31	47.13	54.06	59.21	63.67
	PLOT [5]	45.82	51.32	55.67	61.38	65.29
	KgCoOp [46]	45.46	50.01	53.37	58.38	62.71
	ProGrad [56]	44.19	50.41	54.82	60.31	63.89
	CLIP-Adapter [11]	43.49	44.49	48.95	57.52	62.97
	Tip-Adapter-F [51]	46.92	48.50	57.16	62.38	65.23
	Tip-Adapter-F* [51]	47.68	52.24	56.09	61.05	65.04
	Standard LP [32]	29.63	41.19	51.72	58.78	64.56
	LP++ [19]	46.97	52.44	57.75	62.42	66.40
ProLIP	50.21	54.75	59.30	64.19	68.02	
<i>Caltech101</i>	CLIP (0-shot)			85.84		
	CoOp [55]	87.06	89.14	90.00	91.00	91.77
	PLOT [5]	89.41	90.22	90.69	91.55	92.17
	KgCoOp [46]	88.24	88.85	89.89	90.32	90.93
	ProGrad [56]	88.34	89.01	90.13	90.76	91.67
	CLIP-Adapter [11]	87.69	89.37	90.21	91.33	92.10
	Tip-Adapter-F [51]	87.35	88.17	89.49	90.54	92.10
	Tip-Adapter-F* [51]	88.68	89.36	90.40	91.62	92.63
	Standard LP [32]	68.88	78.41	84.91	88.70	91.14
	LP++ [19]	88.56	89.53	90.87	91.84	92.73
ProLIP	89.25	89.80	91.47	92.37	93.44	
<i>UCF101</i>	CLIP (0-shot)			61.80		
	CoOp [55]	62.80	65.62	68.69	72.57	76.39
	PLOT [5]	63.22	66.49	70.12	74.63	77.39
	KgCoOp [46]	64.37	64.91	68.41	69.86	71.73
	ProGrad [56]	65.13	66.57	69.80	73.01	75.76
	CLIP-Adapter [11]	64.25	66.68	69.77	73.90	77.26
	Tip-Adapter-F [51]	64.28	65.48	67.61	72.05	77.30
	Tip-Adapter-F* [51]	65.50	68.55	70.55	74.25	76.83
	Standard LP [32]	40.80	51.71	61.64	68.47	73.38
	LP++ [19]	65.41	69.20	71.68	74.86	77.46
ProLIP	67.88	70.07	73.51	77.06	79.79	
<i>Flowers102</i>	CLIP (0-shot)			65.98		
	CoOp [55]	69.00	78.47	85.34	91.68	94.47
	PLOT [5]	71.09	81.22	87.61	92.60	95.18
	KgCoOp [46]	68.73	69.63	76.51	80.71	84.48
	ProGrad [56]	72.16	79.55	84.56	91.73	94.10
	CLIP-Adapter [11]	66.86	69.71	77.42	87.20	91.16
	Tip-Adapter-F [51]	67.73	68.18	71.17	84.11	93.02
	Tip-Adapter-F* [51]	78.46	85.14	88.53	92.33	94.26
	Standard LP [32]	56.98	73.40	84.38	91.81	95.05
	LP++ [19]	78.21	84.69	89.56	92.61	94.26
ProLIP	75.33	81.95	88.34	92.68	94.92	

Table 20. **Comparison to state-of-the-art methods.** Average classification accuracy (%) and standard deviation over 10 tasks for 11 benchmarks. Best values are highlighted in bold.

Dataset	Method	$N = 1$	2	4	8	16
<i>StanfordCars</i>	CLIP (0-shot)			55.78		
	CoOp [55]	57.00	58.96	62.81	68.40	72.87
	PLOT [5]	57.47	59.89	63.49	68.75	73.86
	KgCoOp [46]	57.19	58.94	59.85	61.42	62.99
	ProGrad [56]	58.63	61.23	65.02	69.43	72.76
	CLIP-Adapter [11]	56.67	57.94	61.13	65.43	70.24
	Tip-Adapter-F [51]	57.24	58.12	59.34	64.25	71.38
	Tip-Adapter-F* [51]	57.85	60.55	64.22	68.75	74.19
	Standard LP [32]	22.94	35.48	47.49	59.34	69.11
	LP++ [19]	57.20	59.95	63.44	67.81	72.33
ProLIP	58.72	61.71	65.68	70.64	75.64	
<i>FGVCAircraft</i>	CLIP (0-shot)			17.07		
	CoOp [55]	12.50	17.59	21.27	26.85	31.20
	PLOT [5]	17.75	19.55	22.26	26.70	32.09
	KgCoOp [46]	18.61	18.93	21.16	22.80	24.10
	ProGrad [56]	18.41	20.51	23.65	26.98	30.47
	CLIP-Adapter [11]	18.56	19.18	21.00	23.76	33.37
	Tip-Adapter-F [51]	18.23	19.12	20.55	23.60	30.37
	Tip-Adapter-F* [51]	19.08	20.79	23.99	30.58	36.16
	Standard LP [32]	12.66	16.92	21.11	26.53	32.42
	LP++ [19]	19.69	21.58	24.22	27.73	31.73
ProLIP	19.74	22.68	27.08	33.20	39.90	
<i>EuroSAT</i>	CLIP (0-shot)			36.22		
	CoOp [55]	40.36	56.15	66.13	77.02	82.59
	PLOT [5]	44.22	64.19	69.37	78.84	81.76
	KgCoOp [46]	43.86	52.92	59.51	63.23	64.04
	ProGrad [56]	49.37	65.22	69.57	78.44	82.17
	CLIP-Adapter [11]	43.00	48.60	59.15	69.92	75.38
	Tip-Adapter-F [51]	47.63	57.62	69.30	75.22	78.59
	Tip-Adapter-F* [51]	49.27	65.66	70.72	74.66	78.73
	Standard LP [32]	48.29	56.81	64.99	74.56	80.29
	LP++ [19]	57.23	61.65	68.67	75.86	80.53
ProLIP	57.95	70.03	76.48	81.81	85.81	
<i>OxfordPets</i>	CLIP (0-shot)			85.75		
	CoOp [55]	86.27	86.33	85.34	87.85	88.68
	PLOT [5]	87.15	87.23	88.03	88.38	88.23
	KgCoOp [46]	87.51	87.51	88.04	88.59	89.28
	ProGrad [56]	88.34	87.88	88.59	88.87	89.39
	CLIP-Adapter [11]	85.46	86.37	87.21	87.95	88.33
	Tip-Adapter-F [51]	85.70	86.05	86.40	87.66	89.08
	Tip-Adapter-F* [51]	86.05	86.49	87.19	87.89	88.26
	Standard LP [32]	30.62	42.64	55.60	67.32	76.23
	LP++ [19]	84.24	85.74	86.94	87.71	88.38
ProLIP	85.46	86.17	87.05	88.15	89.17	
<i>Food101</i>	CLIP (0-shot)			77.35		
	CoOp [55]	75.58	77.49	77.93	78.92	79.21
	PLOT [5]	77.46	77.72	78.23	78.40	78.86
	KgCoOp [46]	77.20	78.04	77.97	78.39	78.73
	ProGrad [56]	78.36	78.01	78.38	79.11	79.51
	CLIP-Adapter [11]	76.93	77.22	77.64	77.97	78.45
	Tip-Adapter-F [51]	77.53	77.53	77.82	78.26	78.99
	Tip-Adapter-F* [51]	77.58	77.36	77.78	78.17	78.72
	Standard LP [32]	31.59	44.60	56.13	64.45	70.97
	LP++ [19]	76.61	77.22	77.79	78.53	78.88
ProLIP	77.06	77.61	77.74	78.37	79.21	

Table 21. **Comparison to state-of-the-art methods (Continued).** Average classification accuracy (%) and standard deviation over 10 tasks for 11 benchmarks. Best values are highlighted in bold.